Acta Pharmaceutica Sinica B 2018;8(3):320–338

Chinese Pharmaceutical Association
Institute of Materia Medica, Chinese Academy of Medical Sciences

Acta Pharmaceutica Sinica B

www.elsevier.com/locate/apsb
www.sciencedirect.com

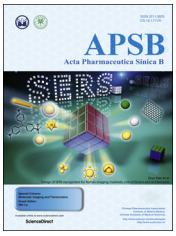

REVIEW

Recent developments in multimodality fluorescence imaging probes

Jianhong Zhao[a], Junwei Chen[a], Shengnan Ma[a], Qianqian Liu[a], Lixian Huang[a], Xiani Chen[a], Kaiyan Lou[a,*], Wei Wang[a,b,]**

[a]*Shanghai Key Laboratory of Chemical Biology, School of Pharmacy, and State Key Laboratory of Bioengineering Reactor, East China University of Science and Technology, Shanghai 200237, China*
[b]*Department of Chemistry and Chemical Biology, University of New Mexico, Albuquerque, NM 87131-0001, USA*

Received 4 February 2018; received in revised form 24 March 2018; accepted 26 March 2018

KEY WORDS

Optical imaging;
Fluorescence;
Multimodality;
Near-infrared fluorescence;
Nanoprobe;
Computed tomography;
Magnetic resonance imaging;
Positron emission tomography;
Single-photon emission computed tomography;
Photoacoustic imaging

Abstract Multimodality optical imaging probes have emerged as powerful tools that improve detection sensitivity and accuracy, important in disease diagnosis and treatment. In this review, we focus on recent developments of optical fluorescence imaging (OFI) probe integration with other imaging modalities such as X-ray computed tomography (CT), magnetic resonance imaging (MRI), positron emission tomography (PET), single-photon emission computed tomography (SPECT), and photoacoustic imaging (PAI). The imaging technologies are briefly described in order to introduce the strengths and limitations of each techniques and the need for further multimodality optical imaging probe development. The emphasis of this account is placed on how design strategies are currently implemented to afford physicochemically and biologically compatible multimodality optical fluorescence imaging probes. We also present studies that overcame intrinsic disadvantages of each imaging technique by multimodality approach with improved detection sensitivity and accuracy.

*Corresponding author. Tel./fax: +86 21 64253299.
**Corresponding author at: Shanghai Key Laboratory of Chemical Biology, School of Pharmacy, and State Key Laboratory of Bioengineering Reactor, East China University of Science and Technology, Shanghai 200237, China. Tel.: +1 505 2770756 Fax: +1 505 2772609.
E-mail addresses: kylou@ecust.edu.cn (Kaiyan Lou), wwang@unm.edu (Wei Wang).

Peer review under responsibility of Institute of Materia Medica, Chinese Academy of Medical Sciences and Chinese Pharmaceutical Association.

https://doi.org/10.1016/j.apsb.2018.03.010

1. Introduction

Precise medical diagnosis and therapy demand sensitive and accurate imaging techniques. In the past few decades, we have witnessed significant improvements in imaging technology in preclinical and clinical translational research and its applications[1]. Optical imaging, particular fluorescence imaging, is widely used in histologic examination of cells, and has gained clinical interest and potential application in intraoperative use[2]. Clinical studies have demonstrated that the optical imaging-guided tissue resection achieves improved removal of cancerous tissue and reduced local recurrence. However, due to photon scattering and light attenuation of biological tissue, fluorescence imaging is limited by depth penetration. It is also difficult to provide quantitative or tomographic information. By combining two or more imaging techniques, multimodal imaging has become an important approach to overcome the limitation of the fluorescence imaging and to achieve noninvasive imaging at greater depths of penetration and higher resolution, and sensitivity required for more accurate diagnosis and delineation of disease lesions[3]. As each imaging modality uses different contrasting agents with distinctive chemical compositions, sizes, solubility, and pharmacokinetic profiles (Supplementary Information Table S1), it is difficult to employ a cocktail approach by using a mixture of various contrast agents together in a single dose while achieve spatiotemporal consistency for all imaging techniques[4]. Therefore, a single probe, which integrates dual or multiple imaging contrasting agents, is preferred for dual- or multimodality imaging applications. In addition, the use of multimodality probe can also reduce toxicity evaluation and pharmacokinetic study workload in preclinical research and reduce the number of quality controls needed during later clinical translational research[3].

Given the recent surge in the amount of scientific literature published concerning these topics, it is a challenging task for us to provide a comprehensive review on this topic. Therefore, this review aims to give a brief account of this emerging research field, emphasizing the strategies used for multimodality fluorescent probe design without delving into details of their biomedical applications. We begin with a brief introduction of advantages and disadvantages of commonly used imaging modalities to help our readers understand the background of each imaging technique and why multimodality optical imaging probes are needed. We then deal with design strategies that were implemented to create physicochemically and biologically compatible multimodality optical fluorescence imaging probes to overcome intrinsic drawbacks of each imaging techniques while achieving improved detection sensitivity and accuracy. More specifically, we focus on multimodality optical fluorescent imaging (OFI) probes that integrate fluorescence reporting groups (fluorophores) with other contrast agents used in X-ray computed tomography (CT), magnetic resonance imaging (MRI), positron emission tomography (PET), single-photon emission computed tomography (SPECT), and/or photoacoustic imaging (PAI). Furthermore, probes that incorporate additional functional moieties such as targeting groups and therapeutic agents are included[5,6]. Case study examples are provided. Finally, we give a summary and our own perspectives of this emerging field.

2. Brief overview of different imaging modalities

2.1. *Optical fluorescence imaging and near-infrared fluorescence imaging*

Optical fluorescence imaging (OFI) using fluorescence microscopy has become one of the most important real-time imaging techniques used to study molecular events in both living cells and *ex vivo* tissue samples. Recently, OFI has been increasingly applied in imaging-guided surgery[7]. The fluorescence reporting groups for OFI include quantum dots[8,9], lanthanide-doped upconversion nanoparticles[10], organic dyes[11], fluorescent proteins[12], aggregation induced emission luminogen[13,14] and etc. Fluorescence emissions in the visible region (400–650 nm) usually have limited utility for *in vivo* imaging applications due to attenuation and scattering of light and interference caused by autofluorescence from endogenous substances such as cytochromes, hemoglobin, and water molecules. Near-infrared fluorescence (NIRF) imaging detects fluorescence emissions in the region of 650–900 nm, has low background tissue absorption for deeper penetration depth, and is more suitable for *in vivo* preclinical and clinical imaging studies[15–18]. Some representative NIR dyes used in multimodality imaging are listed in Fig. 1. Among them, indocyanine green (ICG) is the only NIRF dye approved by Food and Drug Administration (FDA) in the United States for clinical use[19,20]. Another NIR dye, IRDye 800CW, has entered clinical trials[21]. In addition, NIRF imaging in the second biological window (1000–1400 nm), also named over-thousand near-infrared (OTN) imaging, has attracted significant attention in *in vivo* imaging applications due to its even deeper tissue penetration, higher image contrast, and reduced phototoxicity and photobleaching[22]. OTN fluorescence imaging agents include Ag_2S quantum dots[23], rare-earth doped materials[24], Ni-doped magnetic nanocrystals[25], and single-wall carbon nanotube[26].

2.2. *X-ray computed tomography*

X-ray computed tomography (CT) is a technique based on X-ray beam absorbance differences in various tissues, resulting in a three-dimensional anatomic image useful for medical diagnosis of tumors, brain injury, ischemia, and other disease conditions[27]. CT has the advantage of high spatial resolution up to 0.5 mm, unlimited penetration, and fast acquisition of 3D anatomical image. It is also widely available in hospitals and is relatively cost effective. The major limitation of CT is its low soft tissue sensitivity and the lack of functional information. The low sensitivity of soft tissue can be compensated by combined imaging with MRI. More often, in order to increase sensitivity and selectivity and to better discrimination between normal and pathological tissues, CT contrast agents which strongly absorbs X-rays are implemented and include iodinated agents[28], gold nanoparticles[29–31] and TaO_x[32].

2.3. *Magnetic resonance imaging*

Magnetic resonance imaging (MRI) is a versatile imaging modality based upon nuclear magnetic resonance (NMR) in the presence of a strong magnetic field and radiofrequency waves. Images are generated from the differences in longitudinal relaxation time (T_1) and/or transverse relaxation time (T_2) of a specific NMR-active nuclide in different tissues when specially designed radiofrequency pulse sequences are applied[33]. The most common nuclide used in MRI is ^{1}H due to its ubiquitous existence in water molecules in biological systems and its high NMR sensitivity among all nuclei. ^{1}H-MRI can provide 3D anatomical as well as physiological information depending on the specialized MRI technique used. Compared with CT, MRI uses safer non-ionizing radiation and has better spatial resolution for soft tissues. Other merits of MRI include unlimited depth penetration and high spatial resolution. A drawback of MRI is its low sensitivity. Therefore, longer acquisition time and larger amounts of imaging

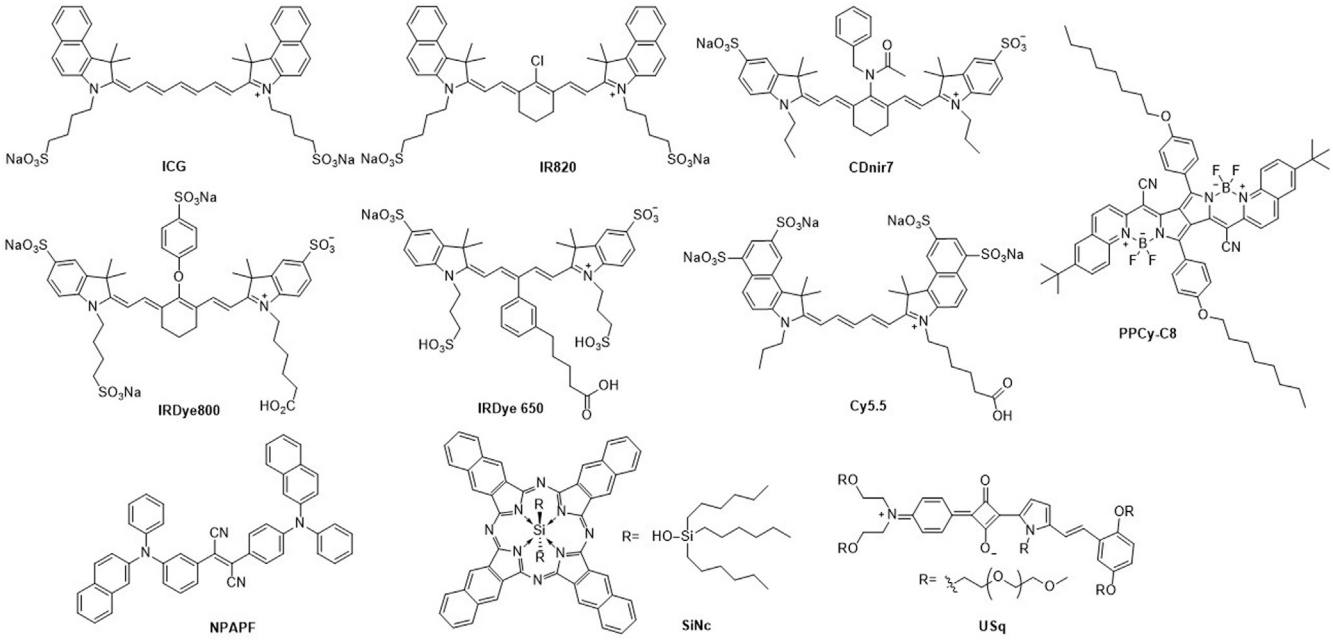

Figure 1 Representative NIRF dyes used in dual-modality optical fluorescence imaging.

agents are often needed. Moreover, MRI contrast agents, such as superparamagnetic iron oxide (SPIO) nanoparticles (NPs), or gadolinium ion (Gd^{3+}) complexes, are employed to disturb the local magnetic field of the targets of interest and to enhance imaging contrast by exerting distinctive proton relaxation effects in tissues: SPIO NPs increases T_2 relaxations and form darker spots in images, while Gd^{3+} paramagnetic complexes decrease T_1 and result in a brighter region. Due to the low sensitivity of MRI imaging, targeted delivery is often adopted to increase signal contrast in the tissue of interest. Alternatively, MRI imaging techniques detecting nuclei other than ^{1}H have also been explored in recent years, particularly ^{19}F-MRI due to its low background and relatively high sensitivity of the ^{19}F nucleus in biological samples[34–36]. Notably, ^{19}F-MRI provides local distributions of ^{19}F atoms more suitable for functional imaging.

2.4. *Positron emission tomography*

Positron emission tomography (PET) is based on the detection of high-energy photon pairs produced during an annihilation collision between a positron and an electron, from which 3D images are reconstructed by computer analysis[37]. PET contrasting agents contain positron-emitting radionuclides, such as ^{18}F, ^{64}Cu, and ^{68}Ga. (Supplementary Information Table S1). These radionuclides typically have short half-lives and are synthesized directly from a cyclotron near the PET imaging facility, where they are chemically incorporated into the structure of PET probes and used immediately to avoid significant decay. Clinically, ^{18}F-labelled imaging agents are used for cancer diagnosis (*e.g.*, [^{18}F]-FDG[38]) and neuroimaging applications (*e.g.*, [^{18}F]-florbetaben for diagnosis of Alzheimer's disease[39]). Notable advantages of PET include unlimited depth of penetration and excellent sensitivity. However, it is a relatively costly procedure and has limited availability due to the requirement of a nearby cyclotron. The main limitation of PET imaging is its low spatial resolution and lack of anatomic reference frames (Supplementary Information Table S1). The low spatial resolution can be compensated by intraoperative optical fluorescence imaging in dual-modality OFI/PET imaging, while additional CT or MRI imaging can provide the anatomic frame in a combined PET/CT or PET/MRI.

2.5. *Single-photon emission computed tomography*

Though similar to PET, single-photon emission computed tomography (SPECT) implements radionuclides which provide 3D images using a different nuclear decay mechanism[40]. The SPECT radioisotopes (*e.g.*, ^{99m}Tc, ^{123}I, and ^{111}In) decay *via* the emission of single γ rays and generally have longer decay half-lives than those of PET. Therefore, they are more convenient to transport for medical use (Table 1)[41]. SPECT is inherently less sensitive than PET, but is less expensive and more clinically available. SPECT also shares similar strengths and limitations with PET, which include unlimited depth penetration, high sensitivity slightly lower than PET, low spatial resolution, and minimal 3D anatomical information (Supplementary Information Table S1).

2.6. *Photoacoustic imaging*

Photoacoustic imaging (PAI), also termed photoacoustic tomography (PAT), is an emerging non-invasive imaging technique[42,43]. When highly absorbed endogenous or exogenous contrast agents within tissue are irradiated by a short laser pulse, the energy absorbed is quickly converted to heat, generating a local pressure increase due to thermos-elastic expansion which then propagates as ultrasonic waves and becomes the photoacoustic signal. Pulsed laser light in near-IR ranges (650–900 nm) is often used because of minimized tissue attenuation in this wavelength region. Because PAI has high spatial resolution (up to 0.15 mm) and deep tissue penetration (up to 7 cm), this imaging technique is a highly effective method to visualize both tissue structure and function. Multispectral optoacoustic tomography (MSOT) is a technology which allows irradiation with multiple wavelengths of laser light and then reconstruction of mixed and/or unmixed PAI images, and is particularly powerful in resolving multiple physiological, morphological, vascular, and molecular features[44,45]. PAI contrast

Table 1 Representative radionuclides for dual-modality OFI/PET and OFI/SPECT probes.

Radionuclide	Imaging modality	Half-life	E_{max} γ (keV)	Representative chelator
^{18}F	PET	109.8 min	640 (97%)[a]	N/A
^{68}Ga	PET	67.6 min	1899 (89%)[a]	DOTA/NOTA
^{64}Cu	PET	12.7 h	657 (18%)[a]	DOTA/NOTA/sarcophagine
^{89}Zr	PET	3.3 d	897 (23%)[a]	DFO
^{111}In	SPECT	2.8 d	245	DTPA/DOTA
^{99m}Tc	SPECT	6.01 h	140	HYNIC
^{177}Lu	SPECT	6.72 h	497	DOTA
^{188}Re	SPECT	16.9 h	155	$(His)(CO)_3$

[a]β^+ purity of the decay.

agents can be modified to include targeting and/or biological stimuli-activatable functions and imaging can be performed using either dual or multiple wavelengths. In addition, PAI has excellent temporal resolution which allows real-time imaging in perfusion kinetics studies of the entire tumor volume[46]. Moreover, PAI contrast agents are often used to convert energy of the absorbed NIR light to heat for photo-thermal therapy (TPP). Overall, PAI is an effective and powerful tool for real-time noninvasive biochemical and functional imaging in preclinical and clinical applications[47]. Compared to optical fluorescence imaging, PAI has relatively less sensitivity due to the limitations of acoustic transducers. Other limitations of PAI include restricted penetration depth while imaging acoustically mismatched tissues, such as bone and lung[48].

3. Design and study of multimodality OFI probes

3.1. *Dual-modality OFI/CT imaging probes*

Since CT imaging provides the 3D anatomical structures which OFI cannot achieve, while OFI offers high superficial resolution and sensitivity in providing biochemical information that CT imaging is lacking, OFI and CT imaging modalities compensates each other. Nonetheless, dual-modality OFI/CT probes face a challenge: they must integrate two imaging agents with distinctive sensitivity. The less sensitive CT requires much larger amount of mass loading of contrast agents for efficient signal readout than does OFI. On the other hand, the requirement of relatively large amount of CT contrast agent further raises the toxicity and/or solubility issues. Biocompatibility and/or targeted selectivity of the dual-modality probe is another issue for probe design. It is often necessary to attach a targeting group for enrichment of CT contrast agent at the desired sites. Considering all the above challenges, targeted nanoprobe-based design is likely the platform of choice for dual-modality OFI/CT probes (Supplementary Information Table S2). Nanoprobes allow entrapment of the CT contrast agents with a protective layer of biocompatible materials, and thus solve problems of toxicity and/or solubility. To compensate the low CT sensitivity, both the loading of CT contrast agents and the size of the nanoprobe are adjustable. It is also convenient to functionalize the nanoprobe with fluorescent agents. Furthermore, conjugation of a large targeting group (*e.g.*, antibody) or multiple targeting group copies on a nanoprobe for targeted delivery of CT contrast agents is possible. CT contrast agents used in recent dual-modality OFI/CT probes included iodinated oil[49], gold nanoparticles[50], Bi_2S_3[51], TaO_x[32], and etc., while various fluorescent materials such as Cy 5.5[49], aggregated AIE dyes[52], Cu-doped CdS quantum dots[53], and persistent luminescence nanoparticles[32] have been adopted as fluorescence reporting groups (Supplementary Information Table S2). To increase the biocompatibility and *in vivo* circulation time for these nanoprobes, PEGylation is often employed[23,51,52]. Typical multilayer construction of a dual-modality OFI/CT nanoprobe is shown in Fig. 2.

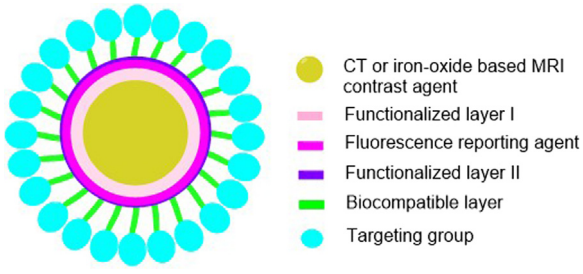

Figure 2 Typical design of a multilayer dual-modality OFI/CT or OFI/MRI (iron-oxide based) nanoprobe. The functionalized layers I and II are for attachment of fluorescence reporting agent or conjugation with additional biocompatible and targeting group.

Qin et al.[23] reported a novel hybrid OFI/CT nanoprobe, Ag_2S-I@DSPE-PEG_{2000}-FA, assembled by mixing Ag_2S QDs and iodinated oil in the presence of distearoylphosphatidylethanolamine-poly (ethylene)-folate (DSPE-PEG_{2000}-FA) and other small molecules in water. Ag_2S QDs emits fluorescence at 1170 nm in the second NIR window with greatly reduced tissue autofluorescence. After injection, the probe was initially enriched in the spleen and then move to the tumor site after 12 h and stayed up to 48 h as indicated from fluorescence and CT imaging (Fig. 3). The low toxicity and long blood circulation time made the nanoprobe particularly suitable for applications such as preoperative investigation and intraoperative imaging. In a second case, Lu et al.[32] developed a NIR persistently luminescent nanoparticle ($Zn_{2.94}Ga_{1.96}Ge_2O_{10}$:$Cr^{3+}$,$Pr^{3+}$, termed ZGGO:Cr,Pr). Excited *in vitro* at 254 nm, and then injected into the living animal for *in vivo* imaging with NIR emission at 695 nm, it was selected as the nanoparticle core to build-up a core–shell nanoparticle covered by a layer of TaO_x shell functioned as CT contrast agent. The outer TaO_x layer was further coated with a layer of modified silica by the reagent 3-aminopropyltriethoxysilane. The synthesized nanoparticles had amine groups on their surface for further convenient conjugation with PEG chains and also cyclic CNGRCGG peptides as the targeting group (Fig. 4). The obtained nanoprobe, NGR-PEG-ZGGO:Cr,Pr@TaO_x@SiO_2 could detect the tumor site in HepG2 tumor-bearing nude mice *in vivo* with either NIRF or CT imaging.

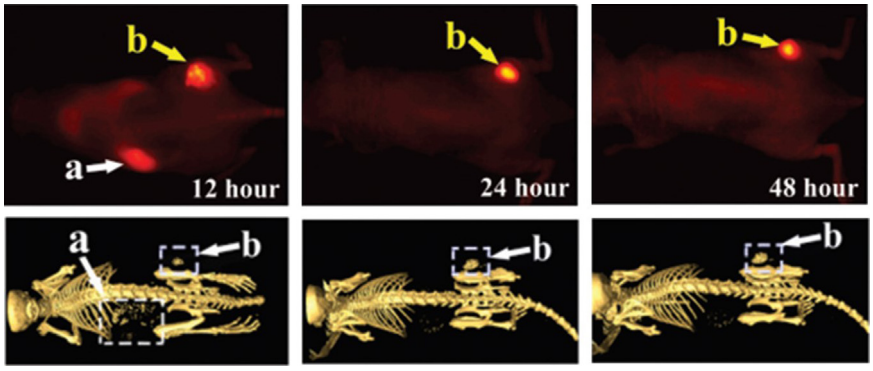

Figure 3 Fluorescence (top) and CT images (below) of nude mice bearing HeLa xenograft tumor 12, 24, and 48 h after tail vein injection of Ag_2S-I@DSPE-PEG_{2000}-FA. Arrow "a" indicates the spleen, while "b" indicates the tumor (Adapted with permission from the Ref. 23. Copyright © the Royal Society of Chemistry, 2015).

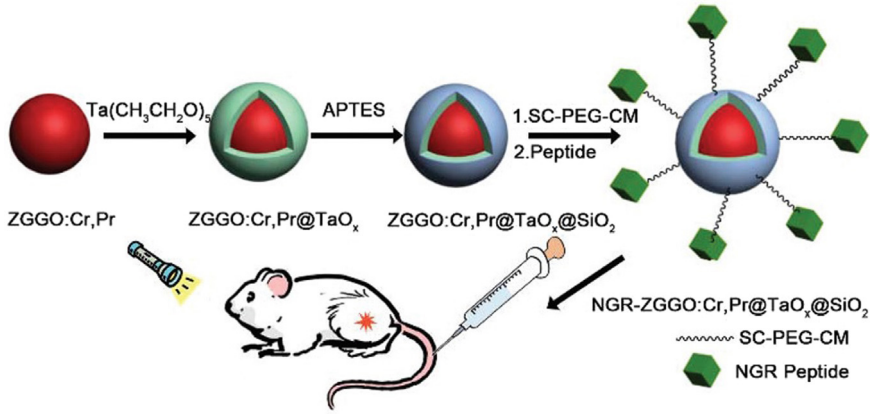

Figure 4 Synthesis of the dual-modality OFI/CT core-shell nanoprobe: NGR-PEG-ZGGO:Cr,Pr@TaO_x@SiO_2 (Adapted with permission from Ref. 32. Copyright © the Royal Society of Chemistry, 2015).

The dual-modality OFI/CT imaging and probe design have attracted research interest since it compensates for limitations of each modality for improved disease diagnosis and treatment. However, these dual-modality probes were relatively less popular compared with other dual- or multimodality imaging probes, likely due to the challenges of finding suitable cost-effective CT contrast agents with high X-ray absorbance, low toxicity, excellent biocompatibility and good stability, and also the right chemistry to link CT contrast agents, fluorescence group, and targeting groups together.

3.2. Dual-modality OFI/MRI and tri-modality OFI/MRI/CT imaging probes

Similar to dual-modality OFI/CT imaging probes, the addition of MRI imaging modality in dual-modality OFI/MRI provides 3D anatomical information which OFI cannot offer, while OFI provides real-time, sensitive, and selective biochemical information which MRI lacks. Compared with CT, MRI is a non-ionizing imaging technique which is safer than CT in terms of ionizing radiation. Moreover, MRI offers much better soft-tissue contrast than CT. The combination of OFI and MRI is one of the most favorable dual-modality combinations (Supplementary Information Table S3). CT modality to enhance bone contrast has been occasionally added to obtain tri-modality OFI/MRI/CT probes. The number of tri-modality OFI/MRI/CT imaging probes has increased in recent years (Supplementary Information Table S4). Challenges are generally associated with the design of dual-modality OFI/MRI probes. First is the inherent difference in sensitivity and since OFI is several orders higher in sensitivity than MRI, more MRI contrast units must be loaded into the probe relative to the number of fluorescence reporting groups to compensate for the low sensitivity of MRI. The second challenge is related to the mismatch of physical properties between the fluorophores and MRI contrast agents; for example, iron oxide is a fluorescence quenching material, therefore, a spacer layer between iron oxide and the fluorophore is necessary for fluorescence signal readout (Fig. 2) and adds significantly to the structural complexity of the probe when additional targeting groups and biocompatible modifications are also considered. Some challenges for multi-modality MRI probe design are related to the inherent properties of the MRI contrast agent. For example, gadolinium complexes are required to stay close to water molecules to give T_1-enhanced MR signals, therefore, they should be stay at the hydrophilic outer surface or hydrophilic inner surface on the nano-holes of a nanoprobe to achieve good signal contrast. Moreover, surface modifications are required to avoid aggregation of the MRI agent because iron oxide nanoparticles tend to aggregate.

Compared with diverse structures of dual-modality OFI/MRI probes ranging from large nanoprobes to small molecules (Supplementary Information Table S3), trimodality OFI/MRI/CT probes were mostly

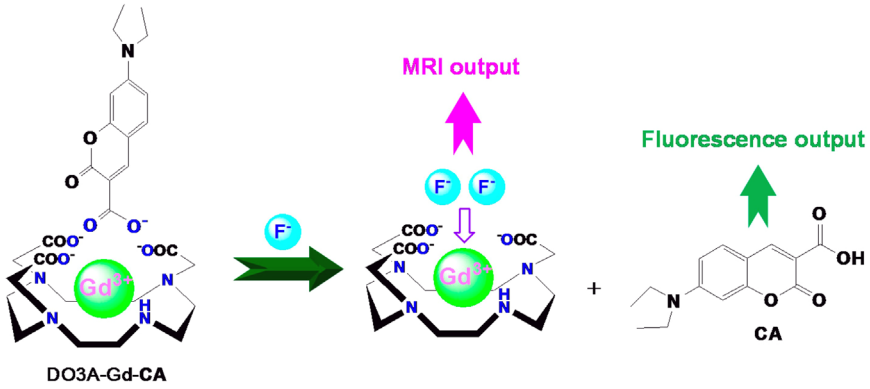

Figure 5 An example of activatable dual-modality OFI/MRI imaging probe for detection of fluorine ion based on Gd(III) complex (Adapted with permission from the Ref. 59. Copyright © 2016 by the reference's authors; licensee MDPI, Basel, Switzerland).

nanoparticle-based, with the exception of one case where the trimodal probe was based on metal organic framework (Supplementary Information Table S4). Although various fluorescent agents were adopted into the dual-modality OFI/MRI or multi-modality probes, the MRI contrasting agents used were limited to three major types: gadolinium(III) ions chelates, iron oxide nanoparticles, and ^{19}F-enriched materials. They have substantial differences in OFI/MRI probe design. Generally, the structural features of an iron oxide based OFI/MRI dual-modality nanoprobe is very similar to that of a typical OFI/CT nanoprobes, shown in Fig. 2. In contrast, Gd(III)-based OFI/MRI dual-modality probes more resemble radio-metal ion-based OFI/PET or OFI/SPECT probes since they share the similarly preinstalled chelating ligands in their structures. ^{19}F-based OFI/MRI probes are structurally diverse, affected by the nature of the ^{19}F-material (*e.g.*, small-molecule or polymer) used.

Stable gadolinium(III) ion complexes containing DTPA (diethylenetriaminepentaacetic acid) or DOTA (1,4,7,10-tetraazacyclododecane-*N*,*N*′,*N*″,*N*‴-tetraacetic acid) are extensively used in clinics[54]. The simple attachment of an organic fluorophore to a Gd(III)'s chelator (DOTA or DTPA) creates a dual-modality OFI/MRI imaging probe[55,56]. However, the 1:1 mol ratio of MRI and optical components resulted in a discrepancy in sensitivity between two imaging modalities. To alleviate this discrepancy, Harrison et al.[57] designed a multimeric NIRF/MRI contrast agent in which a single contrast molecule contains 3:1 mol ratio of Gd complex to NIR fluorophore. The attachment of the NIR-fluorophore resulted in enhanced cell uptake through organic-anion transporting polypeptides (OATPs), also favorable for cell MRI imaging. However, the probe accumulation in the tumors were only detected by OFI, but not MRI, suggesting the necessity for further improvement of the local concentration of MRI contrast agents. Gadolinium(III)-fluorescent dye complexes can also function as activatable MRI and OFI probes for ion detection through ion exchange reaction[58–60]. During the process, the fluorescent dye changes from coordination with Gd(III) to free state or complexation with another metal cation, and generates fluorescence change. An example is shown in Fig. 5. The number of bound water molecules around the Gd(III) ion or the size of the whole complex also varies, resulting in a shift of r_1 value and the T_1-weighted MRI signal. The signal changes in OFI and MRI modalities and therefore gives more reliable detection of the ion of interest. Recently, Wang et al.[59] reported a coumarin dye-Gd(III)-DO3A complex as a dual-modality OFI/MRI probe for fluoride anion detection. The replacement of the coumarin dye by F^- increased the r_1 value from 1.67 to 2.957 $(mmol/L)^{-1}$ s^{-1} and resulted in bright spots in T_1-weighted MRI images in a concentration-dependent manner; a ratiometric response of fluorescence emission from 470 to 460 nm was simultaneously observed.

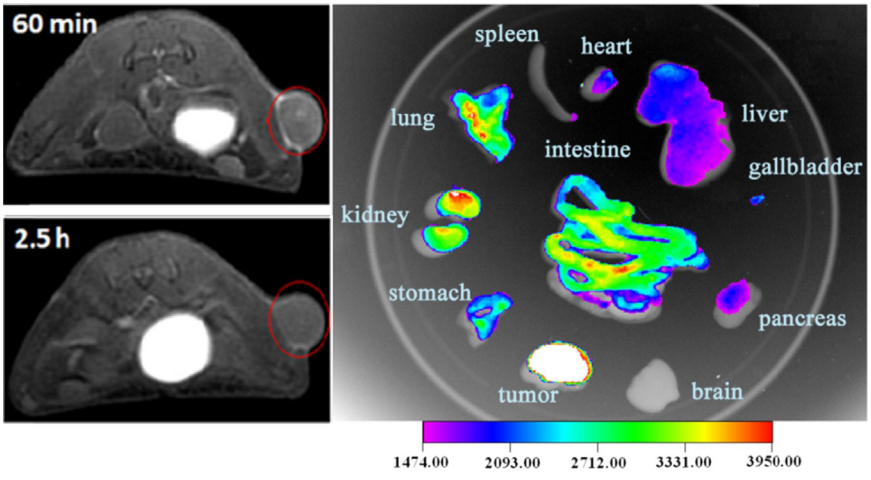

Figure 6 Left: contrast-enhanced MRI images of a nude mouse bearing xenografted KB tumor at time of 60 min and 2.5 h after i.v. injection of the dual-modality OFI/MRI probe PEG-PP-DTPA-Gd^{3+} at a dose of 0.03 mmol/L Gd/kg; right: *ex vivo* fluorescence image of the anatomized organs from the sacrificed mouse at 2.5 h post-injection (Adapted from the Ref. 61 with permission. Copyright © 2016 Elsevier Ltd.).

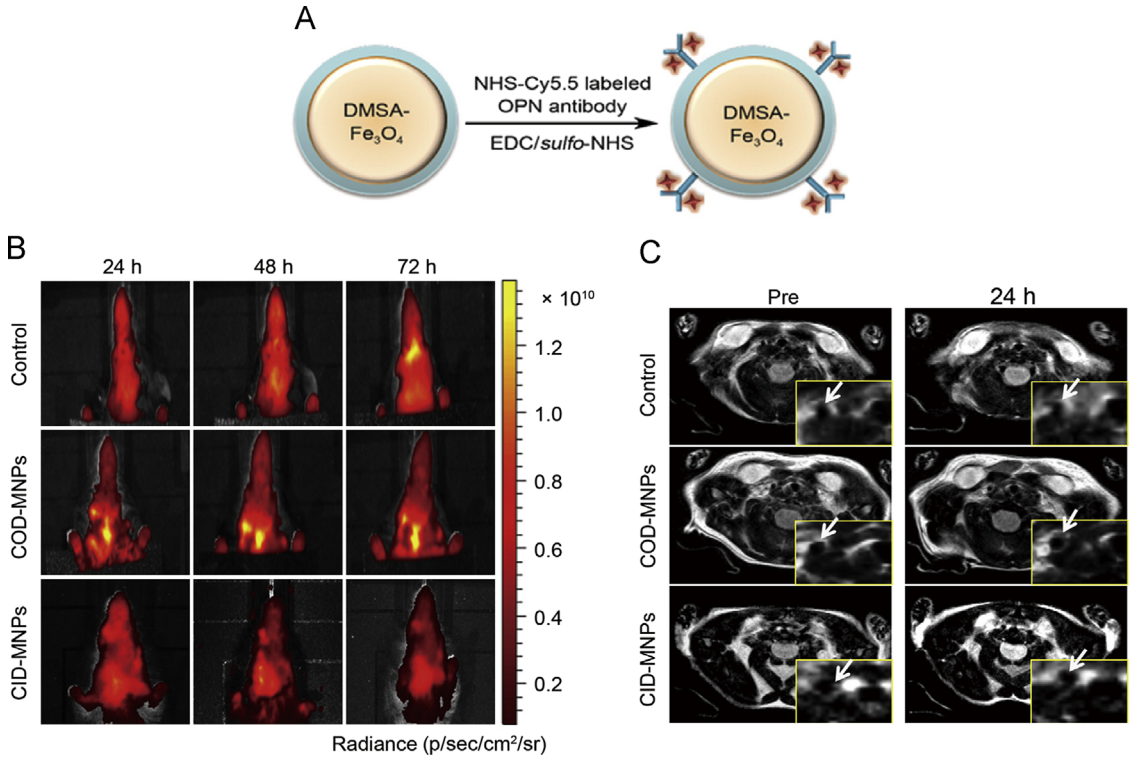

Figure 7 (a) A schematic drawing of preparation of Cy5.5-OPN antibody-labelled iron oxide nanoparticles; (b and c) fluorescence and MR images of high-fat-diet fed mice required at different time point of post-injection of COD-MNPs (the middle line) compared with control images (Adapted from Ref. 65 with permission. Copyright © 2016 Elsevier Ltd.).

More Gd(III)-based dual-modality OFI/MRI probes have been based on nanoprobes or self-assembled polymers (Supplementary Information Table S3). With sizes ranging from six to hundreds of nanometers, they are larger and have longer circulation times than do small-molecules. The larger sizes also allowed them to be loaded with more MRI contrast agents and obtain much higher r_1 values. For example, Hu et al.[61] reported a star-like polymer PEG-PP-DTPA-Gd^{3+} with a porphyrin ring at the center as a NIR fluorophore and was labelled with Gd(III) chelates at polymeric arms. The probe has an enhanced r_1 value of 7.1 $(mmol/L)^{-1}$ s^{-1}, 1.6 times higher than that of the Gd(III)-DTPA complex, likely due to the increased rotational correlation time. The *in vivo* MRI images of a nude mouse bearing xenografted tumor clearly showed the boundary of a tumor, 60 min after the injection of the probe (Fig. 6, left). The enrichment of the probe on the surface of the tumor was further verified by *ex vivo* fluorescence imaging (Fig. 6, right), indicating it had excellent tumor-targeting capability likely because of an enhanced permeability and retention (EPR) effect. Even higher r_1 value could be achieved on the nanoprobe design. Zhu et al.[62] prepared mesoporous silica nanoparticles (MSN) with functionalized amine groups on their surface for dual-labelled with NIR dye IR 808 and Gd-DTPA. Synthesized dual-modality imaging probes have an average particle size about 120 nm. Remarkably, the MSN-based probe had a r_1 value of 14.54 $(mmol/L)^{-1}s^{-1}$ and an excellent NIR fluorescence profile. In addition, the probe also showed excellent biocompatibility and high intracellular retension ability.

Different from T_1-weighted Gd(III) chelates mentioned above, another major class of MR contrast agents, the iron oxide nanoparticles, is T_2-weighted for MRI contrast[63]. These

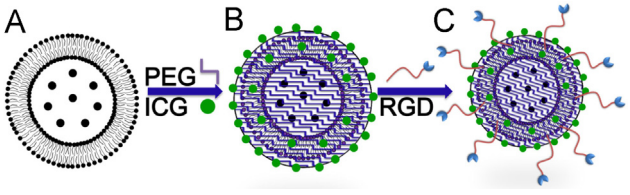

Figure 8 Schematic representation of the synthesis of SPIO@liposome-ICG-RGD (Adapted from Ref. 66 with permission. Copyright © 2017 by authors under Creative Commons).

nanoparticles are often coated with a biocompatible layer to prevent aggregation in biological systems. The separating layer also functions to keep fluorophore molecules from being quenched and as conjugation sites for attachment of targeting groups and/or therapeutic drugs. In a recent report by Yan et al.[64], super-paramagnetic iron oxide (SPIO) was surface-functionalized and conjugated with the Cy5.5-labelled peptide GX1, an angiogenesis-related marker of gastric cancer. The targeted probe was enriched in tumor at concentrations much higher than those in other organs except for the liver, as indicated from *in vivo* optical imaging. It also gave dark contrast spots in MR images at the tumor site. Similarly, iron oxide nanoparticles surface-coated with *meso*-2,3-dimercaptosuccinic acid (DMSA) was conjugated with Cy5.5-labelled osteopontin (OPN) antibody. The targeted dual-modality OFI/MRI probe obtained, Cy5.5-OPN-DMSA-MNPs (COD-MNPs), was used for *in vivo* tracking of vulnerable atherosclerotic plaques in an atherosclerosis model of high-fat-diet fed mice and compared with the other two imaging conditions (Fig. 7)[65]; one condition employed normally fed mice instead of high fat diet (HFD) fed mice, the other used a non-targeted dual-modality

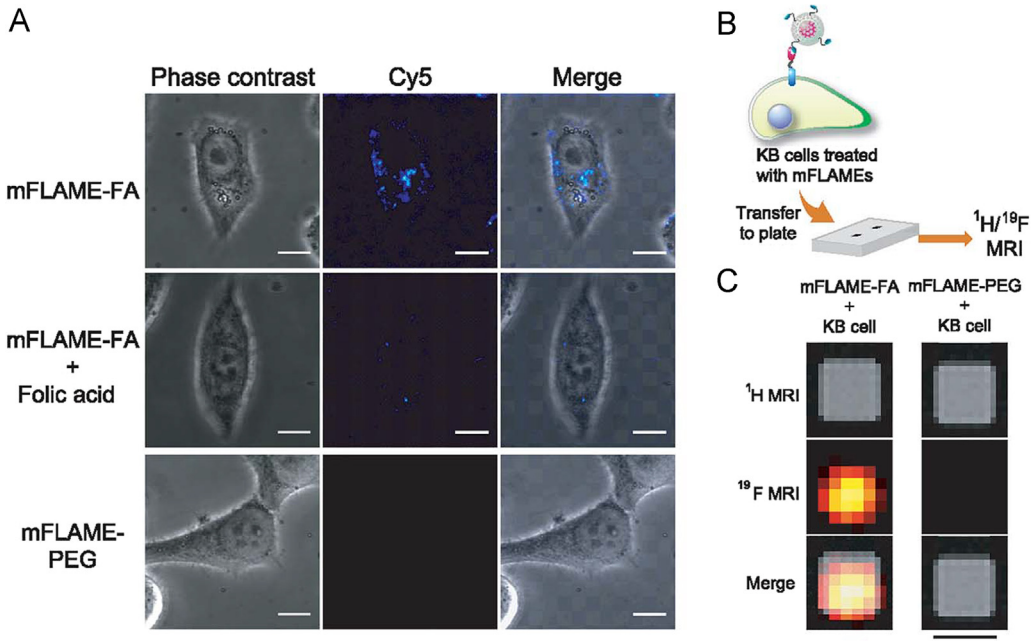

Figure 9 (a) Confocal fluorescence microscopy images of KB cells treated with mFLAME–FA or mFLAME–PEG with or without folic acid for 4 h. (λ_{ex} = 635 nm and λ_{ex} = 660–760 nm, Scale bar: 10 μm); (b) Illustration of the experimental procedure for the MRI detection of mFLAME–FA in KB cells; (c) $^{1}H/^{19}F$ MR images of KB cells treated with mFLAME–FA or mFLAME–PEG. The matrix size was 64 × 64, slice thickness was 30 mm, and RARE factor was 16. $T_{E,eff}$ and T_R were 40 and 1000 ms, respectively. The number of average was 128. The acquisition time is 34 min 20 s. Scale bar: 0.3 μm (Adapted from the Ref. 67 with permission. Copyright © 2015 the Royal Society of Chemistry).

probe, Cy5.5-IgG-DMSA-MNPs (CID-MNPs) based probe, as control probe in which OPN antibody was replaced by an IgG antibody. Fluorescence images revealed much higher fluorescence intensity of the plaques in carotid artery of the HFD fed mice compared with that of either the normally fed group (control group) or the non-targeted HFD fed group (CID-MNPs). The T_2-weighted MRI images also indicated darker spots in non HFD fed mice where plaques were located. The imaging results not only suggested the potential use of the dual-modality OFI/MRI probe for imaging of the vulnerable atherosclerotic plaques, but also provided an example in which both fluorescence imaging and active targeting compensate for MRI low sensitivity[65]. Recently, in another report by Chen et al.[66], the dual-modality OFI/MRI was constructed from SPIO nanoparticles coated with functionalized liposomes containing PEG, a tumor-targeted peptide (RGD), and ICG (Fig. 8). The probe demonstrated its utility in preoperative diagnosis and intraoperative resection guidance in a mouse model bearing both orthotropic liver tumors and intrahepatic tumor metastasis. The probe was able to detect small tumors with sizes of 0.9 ± 0.5 mm with MRI, effective for preoperative diagnosis. Active targeting capability and long clearance rate allowed fluorescence imaging to detect miniscule tumor metathesis lesions as small as 0.6 ± 0.3 mm at a 72 h time point post-injection.

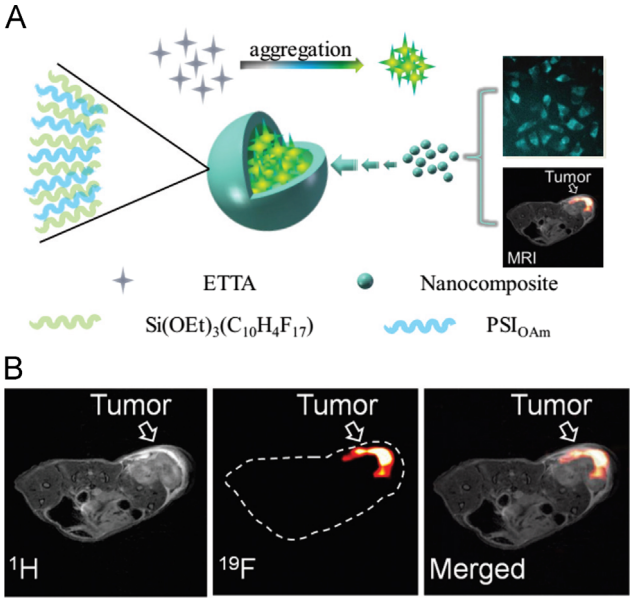

Figure 10 (a) Fabrication of ETTA@PSIOAm–PDTES nanocomposites for dual-modality OFI/MRI; (b) *in vivo* ^{19}F-MRI and ^{1}H-MRI of the tumor-bearing mice with RGD-conjugated ETTA@PSIOAm–PDTES nanocomposites (Adapted from the Ref. 68 with permission. Copyright © 2017 the Royal Society of Chemistry).

Recently, ^{19}F-enriched material, a third major class of MRI contrast agents, was also investigated for use in construction of dual-modality OFI/MRI imaging probes[35,67–69]. Goswami et al.[69] constructed a B_{12}-based dual-labelling platform with a precise mole ratio of 11:1 of MRI contrast groups (a total 66 ^{19}F atoms) to the fluorophore (sulforhodamine-B) in order to compensate the relatively low sensitivity of MRI versus OFI. The study did not test the probe in MR imaging. Nakamura et al.[67] reported a core-shell nanoprobe mFLAME–FA with a perfluorocarbon-based core and a mesoporous silica shell. The shell was labelled with both the fluorescence dye (Cy5) and the targeting group folic acid (FA). The probe was also loaded with anticancer drug doxorubicin (DOX) in the mesoporous silica layer and converted to a theranostic probe with both cancer diagnosis and therapy capabilities. *In vitro* fluorescence and ^{19}F-MRI images of KB cells clearly showed the targeting group was necessary for effective labelling (Fig. 9).

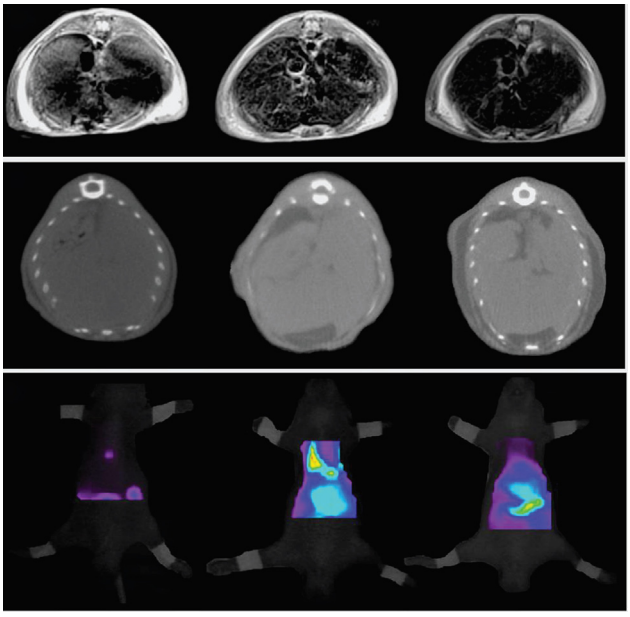

Figure 11 *In vivo* imaging of i-fmSiO4@SPIONs. (A) T_2-weighted MR, (B) CT, (C) fluorescence images of mouse livers after intravenous injection of i-fmSiO4@SPIONs (Adapted from Ref. 72 with permission. Copyright © 2014 by the Ref. authors under Creative Commons).

Notably, combination of ^{1}H- and ^{19}F-MRI is able to provide both anatomic and whole body functional imaging noninvasively. An example was seen in recent work by Guo et al.[68]. Aggregated 4,4′,4″,4‴-(ethene-1,1,2,2-tetrayl)tetraaniline (ETTA) used as a fluorescent reporting group was encapsulated with oleylamine modified polysuccinimides (PSI_{OAM}) and 1*H*,1*H*,2*H*,2*H*-perfluorodecyltriethoxysilane (PDTES) to obtain the ETTA@PSIOAm–PDTES nanocomposite and subsequently conjugated with the targeting group RGD peptide. The probe was successfully used in fluorescence imaging of HeLa cells and *in vivo* ^{1}H- and ^{19}F-MRI imaging of 4T1 cancer cell xenograft mice (Fig. 10)[68].

Compared with dual-modality OFI/MRI or OFI/CT probes, tri-modality OFI/MRI/CT are more challenging to design because it is simply difficult to integrate three different contrast agents with distinctive properties into a single nanoprobe assembly without affecting individual function. Most tri-modality imaging probes have employed Gd(III) complexes as the MRI contrast agents (Supplementary Information Table S4). Only a few of them have been based on superparamagnetic iron oxide nanoparticles[70–73].

In vivo images of a representative tri-modality OFI/MRI/CT nanoprobe are shown in Fig. 11[72]. The probe, iodinated oil-loaded fluorescent mesoporous silica-coated superparamagnetic iron oxide nanoparticles (i-fmSiO4@SPIONs), was constructed using superparamagnetic iron oxide nanoparticle (SPIONs) as the core and using Cy5-functionalized mesoporous silica as the shell loaded with iodinated oil as the CT-contrast agent. The nanoprobe was also surface-modified with PEG to increase bioavailability and blood circulation time[72]. From images, MRI clearly provided much better anatomical resolution of soft tissue than did CT imaging and CT imaging gave better contrast of bone than did MRI. Though fluorescence images had the lowest spatial resolution among the three, they provided the highest contrast in terms of spot brightness indicating high sensitivity of OFI imaging. The combination of the three modalities compensates the limitations of each modality and provides more complete and accurate delineation of anatomical and functional structures of the target tissue of interest.

So far, most of the tri-modality OFI/MRI/CT probes have been developed for cancer or tumor diagnosis and delineation. Their compositions are diverse and complex, due to various combinations of OFI, MRI, and CT contrast agents (Supplementary Information Table S4). In a few cases, additional therapeutic capabilities were also explored[71,73–76]. Often, one contrast agent adopted in a tri-modality probe happened to have additional therapeutic photodynamic or photothermal properties. Wu et al.[74] reported a liposome-based multifunctional nanoprobe, in which IR820 (a NIRF dye), Gd-DOTA (a MRI contrast agent), and Iohexol (a CT contrast agent), and ammonium bicarbonate (NH_4HCO_3) were encapsulated inside the inner cavity *via* self-assembly. Liposomes averaging between 104 and 135 nm in size were obtained by the extrusion method. The NIR dye IR820 functioned not only as fluorescence reporting group, but also was responsible for the light-triggered release of trapped contrast agents. The process began with energy absorption from the 808 nm NIR laser light and conversion to heat by the dye IR820, which in turn caused the temperature of the inner liposome cavity to rise and the decomposition of NH_4HCO_3 to generate CO_2 gas. Generated CO_2 bubbles ruptured liposomal structures and released all the contrast agents (Fig. 12)[74]. Notably, the released dye IR820 emitted stronger fluorescence emission than when kept inside the nanoprobe, due to self-quenching effects at higher concentrations inside liposomes. The MRI and CT signals were also enhanced at the tumor sites after the photo-triggered release. The probe therefore functioned as a photo-activated multimodality imaging agent. Notably, IR820 was effective as a photo-thermal

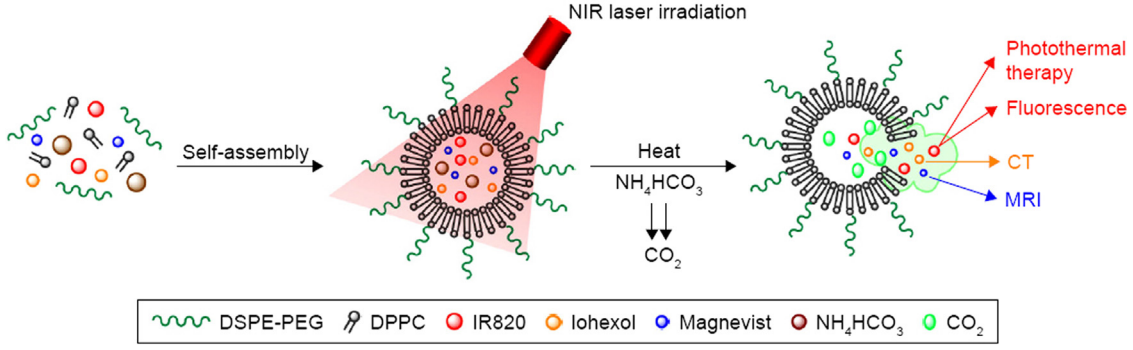

Figure 12 Schematic illustration of light-triggered nanoprobe for tri-modality OFI/MRI/CT imaging and photothermal therapy (Adapted from Ref. 74 with permission. Copyright © 2017 by the reference's authors under Creative Commons).

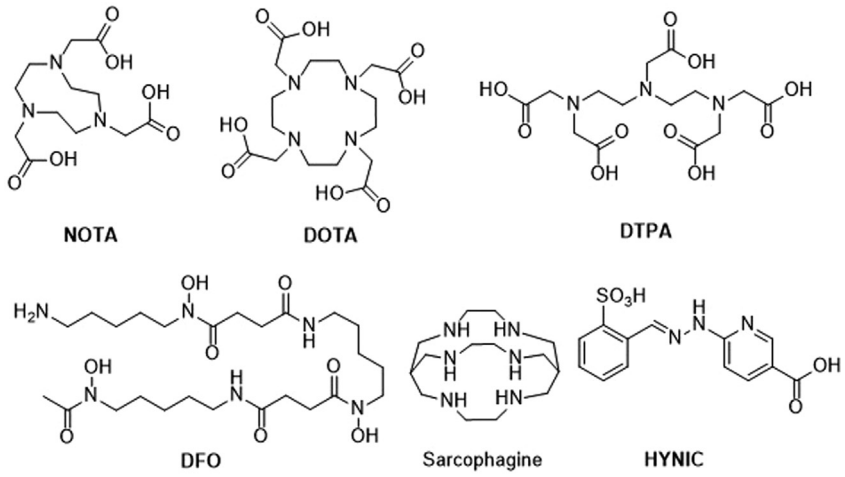

Figure 13 Representative chelating groups for radiometal ions used in multi-modality fluorescent probes.

agent for ablation of tumor cells when it completely inhibited C6 tumor growth in nude mice up to 17 days after NIR laser irradiation. In the future, similar light-triggered nanotheranostics system with both multimodality imaging and cancer therapy capabilities will certainly be used when additional spatial and temporal controls are required.

The addition of MRI imaging modality provides noninvasive and non-radiative 3D anatomical or functional images with high spatial resolution and deep-penetration that traditional OFI imaging cannot achieve. On the other hand, the low sensitivity of the MRI imaging as well as the long acquisition time could be partially compensated by the real-time capability of the fluorescence imaging. There are certainly advantages for a combined use of OFI and MRI, particularly in a clinic scenario when preoperative investigation is performed by MRI while using OFI during surgical operation for delineation of small lesions not identified in MRI. The wide availability of MRI instruments and well-developed MRI techniques make both dual-modality OFI/MRI and tri-modality OFI/MRI/CT the most reported among multimodality imaging probes and techniques. However, their full potentials have yet to be explored. For example, active targeting groups have not yet added to current tri-modality OFI/MRI/CT probes (Supplementary Information Table S4). We would expect to see further progress for targeted dual- or multi-modality OFI/MRI imaging probes.

3.3. *Dual-modality OFI/PET imaging probes*

The combination of OFI/PET imaging modalities offers a highly compensatory and synergistic way for visualization and diagnosis of disease lesions, since PET allows non-invasive, quantitative, and extremely sensitive *in vivo* imaging without penetration limitation, and OFI offers low cost, convenient operation, multi-plexing capability, and high spatial resolution at histologic or superficial levels[77,78]. The OFI/PET dual-modality probes are therefore promising tools in clinical preoperative PET imaging and intraoperative optical imaging-guided surgery. Since both imaging techniques have comparable sensitivity, equal mole ratios of each signal agent are generally satisfactory for both OFI and PET imaging. Another advantage of the dual-modality OFI/PET imaging probe is that due to the high sensitivity of each modality and because only a trace amount of the imaging probe is needed, chemical toxicity is generally not a serious issue.

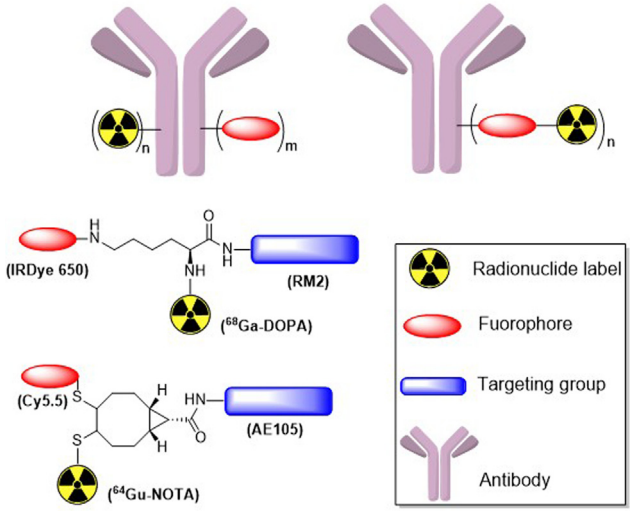

Figure 14 Representative designs of dual-modality OFI/PET or OFI/SPECT probes with radiometal ions.

To design a dual-modality OFI/PET probe, NIR dye and especially cyanine-based NIR organic dye (Fig. 1), is preferred for its relatively deeper tissue penetration[79]. Fluorophores with emission wavelengths in the visible region are also tolerated, since fluorescence imaging is partially compensated by PET with unlimited depths of penetration. PET tracers are positron-emitting radionuclides such as ^{18}F, ^{64}Cu, and ^{68}Ga. There properties are shown in Table 1. Among them, ^{18}F labeling is generally achieved by chemical synthesis starting from readily available ^{18}F anion[80]. Radiometal ions are introduced by a two-step process: an initial pre-installation of a metal chelator by chemical synthesis and a later chelating step with the radiometal ion[81]. Each radiometal ion has its own preferred chelators (Table 1 and Fig. 13). Other specifically designed chelators can also be considered after careful study of the chelating conditions and bio-stability. The choice of the radiometal ion and its chelator pair largely determine the chelation reaction conditions such as temperature, time, ratios of radio-labeling, and also the *in vivo* stability of the chelate. The choice may also affect the receptor binding properties of a targeted multifunctional probe[82]. Another important consideration for the choice of PET radionuclide is the biological event to be tracked. The half-life of positron-emitting radionuclide for labelling must correlate with biological events of interest; otherwise, the obtained image may not truly reflect the spatial distribution of the target event. For example, ^{18}F has a relatively short half-life of 109.8 min and is best used for labelling small molecules having fast clearance rate, while ^{64}Cu with a half-life of 12.7 h could be used to track monoclonal antibodies for up to 48 h[83].

Another important consideration during dual-modality OFI/PET probe design is related to the targeting group. Since PET imaging detects the distribution of the radionuclides, any nonspecific binding or ion-leakage of the probe would generate non-targeted signal or artifacts. An example of comparison of targeted and nontargeted images is given in Fig. 15. Generally, targeting group is necessary to improve accuracy in PET detection by reducing the nonspecific binding (Supplementary Information Table S5). The target group also affects double-labelling strategies used in construction of the dual-modality probes (Fig. 14). Depending on the sizes of the targeting group and the availability of the multiple conjugations sites, OFI/PET dual-modality imaging probes fall into three major categories: dual-labelled monoclonal antibodies (mAbs), dual-labelled peptides, and dual-labelled small biomolecules (Supplementary Information Table S5).

Antibodies have multiple reactive sites when labelled with PET tracer atoms and fluorescence reporting groups. For most of dual-labelled antibodies, PET chelating groups and fluorophore molecules have been conjugated to the antibody sequentially. It has been difficult to control the exact number of chelating groups and fluorophore molecules in a single antibody molecule in molar ratios, as shown in the top-left structure in Fig. 14[84–86]. In an alternative approach, the ratio of the fluorescence reporting group to the PET tracer was fixed to 1:1 by first linking the OFI reporting group and PET tracer together, and then attaching to the antibody through a single conjugation step, as shown in the top-right structure in Fig. 14. The number of double-labelling moieties may still vary in individual antibody molecules. Further improvement resorts to a site-specific labelling technique which uses homogeneously double-labelled mAbs in dual OFI/PET imaging[87]. For targeting groups smaller than mAbs, such as peptides or other small biomolecules, a multivalent linker is often employed to place all the imaging tracers and targeting groups together, as shown in the bottom structures in Fig. 14. The most popular linker group is lysine. A typical design is to conjugate the targeting group with the carboxylic acid of the lysine and then link the chelator and the NIR fluorophore to the two amino groups. In a recent example, Zhang et al.[88] constructed a NIRF-PET dual-modality imaging probe for prostate cancer by linking the targeting group RM2, a nonopeptide specifically binding to gastrin-releasing peptide receptors, with the chelating group (DOTA) and the NIR fluorophore (IRDye 650, Fig. 1) *via* the lysine, as shown in the bottom-middle structure in Fig. 14. Click chemistry was also adopted for facile construction of dual-modality probes. For example, recently, Sun et al.[89], reported to use a strained cyclooctyne, bicyclo[6.1.0]nonyne (BCN), as the linker for a quick assembly of a targeted dual-modality PET/NIRF probe, ^{64}Cu-CHS1. Firstly, AE105, a small linear peptide with high binding affinity for urokinase-type plasminogen activator receptor (uPAR), was linked to BCN through the amide bond. Then the PET chelator (NOTA) and NIRF fluorophore (Cy5.5) were conjugated sequentially through

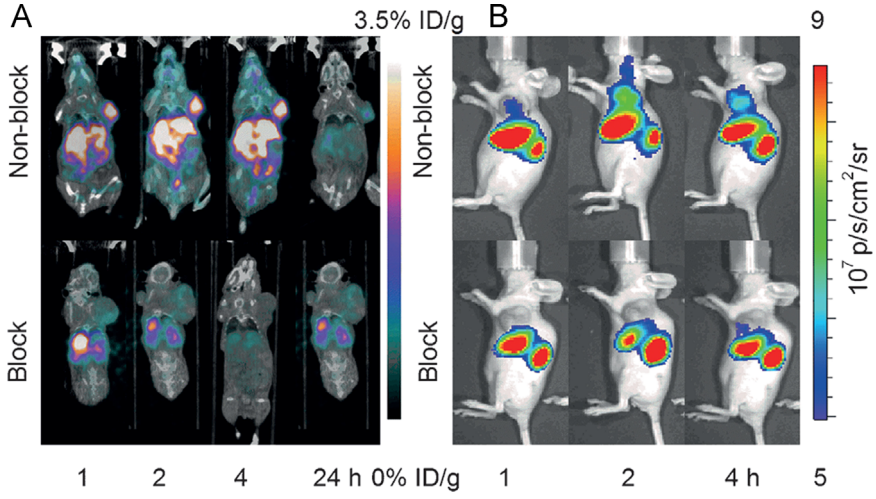

Figure 15 A) The PET/CT images of U87MG-tumor-bearing mice (red rings indicate the location of the tumor, $n = 4$ per group) acquired at 1, 2, 4, and 24 h after tail vein injection of ^{64}Cu-CHS1 with and without the blocking agent AE105. B) The fluorescence images of U87MG tumors at 1, 2, and 4 h after tail vein injection of ^{64}Cu-CHS1 with and without the blocking agent AE105[89] (Adapted from the Ref. 89 with permission. Copyright © 2015 Wiley-VCH Verlag GmbH & Co. KGaA, Weinheim).

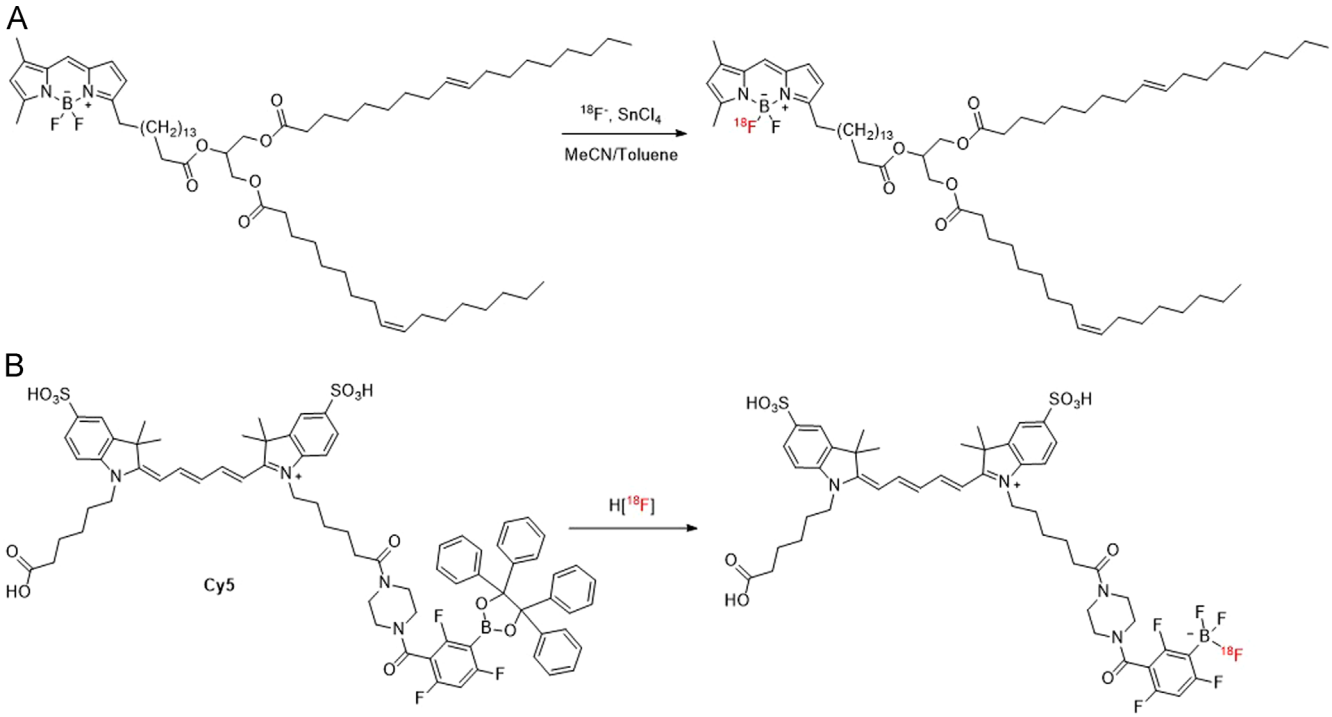

Scheme 1 Representative synthetic schemes of dual-modality OFI/^{18}F-PET probes. (A) Synthesis of an ^{18}F-labelled BODIPY-C_{16}/triglyceride[91]. (B) Synthesis of an ^{18}F-labelled cyanine dye using boronateas as the ^{18}F-trapping group[92].

double base-catalyzed thiol-addition reactions to the strained triple bond in the BCN moiety to create the dual-modality probe, as shown in the bottom left structure in Fig. 14. The NIRF/PET imaging studies showed that the probe ^{64}Cu-CHS1 has excellent tumor uptake, high tumor contrast, and good specificity in the U87MG-tumor-bearing mice model (Fig. 15)[89], suggesting that the BCN moiety is a viable linker for click-chemistry based assembly of targeted dual-modality imaging probes. In another study, Sun et al.[90] reported a new strategy to prepare dual-modality OFI/PET imaging probes using alkene-tetrazole photo-click chemistry to introduce a targeting group and simultaneously form a fluorophore. To demonstrate proof-of-principle, the uPAR- and EGFR-targeted dual-modality probes were prepared *via* this new strategy and the probe was able to perform cell fluorescence staining and PET imaging in the xenograft tumor mice model. However, the *in vivo* fluorescence imaging capability of their probes were limited by the short fluorescence excitation wavelength of the pyrazoline fluorophore formed. Considering further advances in the field of biocompatible click chemistry and conjugation methodology, we expect more diversified double-labelling strategies will emerge for the synthesis of dual- or multi-modality targeted imaging probes.

One drawback of radiometal tracers is the inherent bulkiness of the metal-chelator complex, which may affect the probe's interaction with its biological target. The small size of ^{18}F atom gives minimal structural perturbations, and ^{18}F is currently the most popular radionuclide for clinical PET. For dual-modality OFI/PET

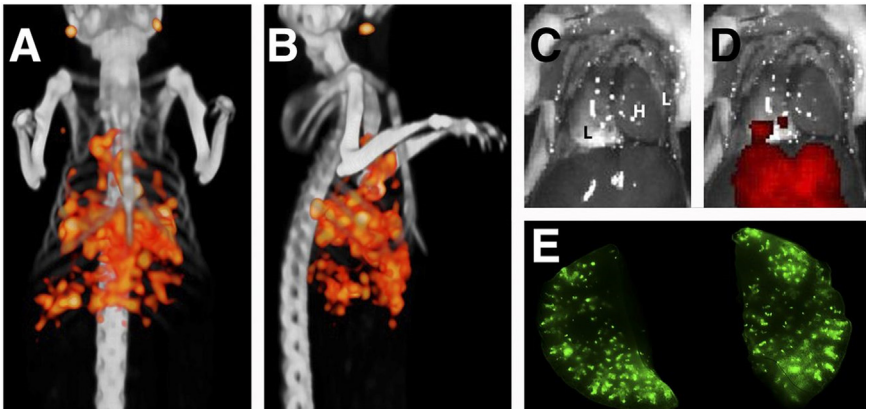

Figure 16 Dual-modality NIRF/SPECT imaging in GW-39 xenograft mice pulmonary tumor model. (A and B) SPECT/CT imaging of pulmonary tumors on coronal (A) and sagittal (B) views; (C) No tumors were visible to the naked eye (L:lung; H:heart); (D) Fluorescence imaging showed superficial tumors; (E) Fluorescence imaging of resected lungs showed numerous tumor lesions (Adapted with permission from the Ref. 101. Copyright © 2017 the Society of Nuclear Medicine and Molecular Imaging).

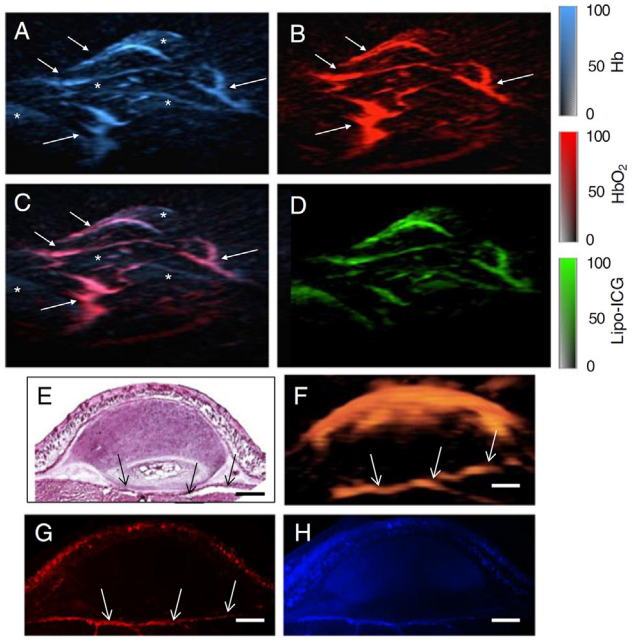

Figure 17 Dual-modality *in vivo* NIRF/MSOT imaging of a 4T1 breast tumor (xenograft mice model) 10 minutes post lipo-ICG injection. Spectrally-unmixed distribution of oxygenated (HbO_2) and deoxygenated haemoglobin (Hb) are shown in (a) and (b), respectively; (c) Superimposition of the HbO_2 and Hb maps; (d) Distribution of the lipo-ICG agent unmixed from the multispectral data; (e) Haematoxylin-eosin staining for tumour cryo-section; (f) A single 2D cross-section from the volumetric data acquired *in vivo* by the vMSOT system from a tumour allograft after performing unmixing for the presence of lipo-ICG; (g) Fluorescence microscopy of lipo-ICG fluorescence; (h) Fluorescence microscopy of the same section stained with DAPI. Arrows point to major blood vessels. Asterisks define predominantly Hb-rich areas formed in part due to blood infiltration into the tumor mass through leaky vessels. Color scales represent the corresponding chromophore concentrations in arbitrary units (Adapted with permission from the Ref. 46. Copyright © 2015 the European Society of Radiology).

imaging probes, the radionuclide can be incorporated through $^{18}F/^{19}F$ exchange or ^{18}F trapping reactions. The $^{18}F/^{19}F$ exchange reaction of the BODIPY fluorophore provides a straightforward way to endow a fluorescent dye with dual-modality functions without chemical structure modifications[85]. Paulus et al.[91] synthesized an ^{18}F-labelled BODIPY-C_{16}/triglyceride (Scheme 1A) through $^{18}F/^{19}F$ exchange reactions in the presence of $SnCl_4$. This probe has demonstrated as a dual-modal fluorescence/PET probe for selective detection of the distribution of brown adipose cells *in vitro* and *in vivo* and possibly will elucidate yet unclear roles of brown adipose tissue during whole body energy metabolism. For fluorophores which do not have exchangeable fluoride atoms in their structures, a potential solution for [^{18}F]-labelling is to conjugate a fluorine trapping group to the fluorophore, similar to the appendance of a chelator group to trap radiometal cations. A typical example was seen in recent work by An et al.[92], in which a boronate was used as the F-trapping group and was conjugated to the NIR dye Cy5 by amidation. The boronate was then conveniently converted to arylboron trifluoride in the presence of H[^{18}F] to achieve ^{18}F-labelling (Scheme 1B). The probe identified a tumor site by PET imaging in an A549 tumor xenograft mice model. During ^{18}F-labelling, the synthesis and purification process must be fast, efficient, and amenable to automation process using readily available ^{18}F-source because of the short half-life of ^{18}F (110 min). The emergence of modern synthetic methodology for ^{18}F labeling greatly expands the scope of the molecular substrate of ^{18}F-PET and will certainly accelerate investigation and development of the dual-modality OFI/^{18}F-PET imaging probes.

Currently, most OFI/PET dual-modality probes are developed for use in oncology because of their potential translation to clinic in cancer diagnosing, staging and therapy monitoring (Supplementary Information Table S5)[77]. Other biomedical research fields including brown adipose tissues[91], intracranial hemorrhage and damage[93,94], myocardial perfusion[95,96] and Alzheimer's disease[97] have also considered dual-modal probe use in their preclinical studies in order to unravel or track the physiological or pathological changes inside the body. With both the upsurge in development of synthetic labelling methodology and the expansion of biomedical applications, we expect advancement of use of the dual-modality OFI/PET probe in translational medicine in the near future.

3.4. *Dual-modality OFI/SPECT imaging probes*

Similar to dual-modality OFI/PET imaging probes, dual-modality OFI/SPECT probes combine advantages of OFI's convenient, real-time, and high resolution superficial imaging ability together with SPECT's high penetration ability, excellent sensitivity, and quantitative signals. Probe design is also very similar, except that γ-emitting radioisotopes such as ^{99m}Tc and ^{111}In are used[79]. For recently reported dual-modality OFI/SPECT probes, the most frequently adopted SPECT radionucleus was ^{111}In (Supplementary Information Table S6) and the preferred fluorescence reporting groups were cyanine-based NIR dyes (Fig. 1). Targeting groups were generally employed to enhance the contrast for the disease lesions or biological events of interest (Supplementary Information Table S6).

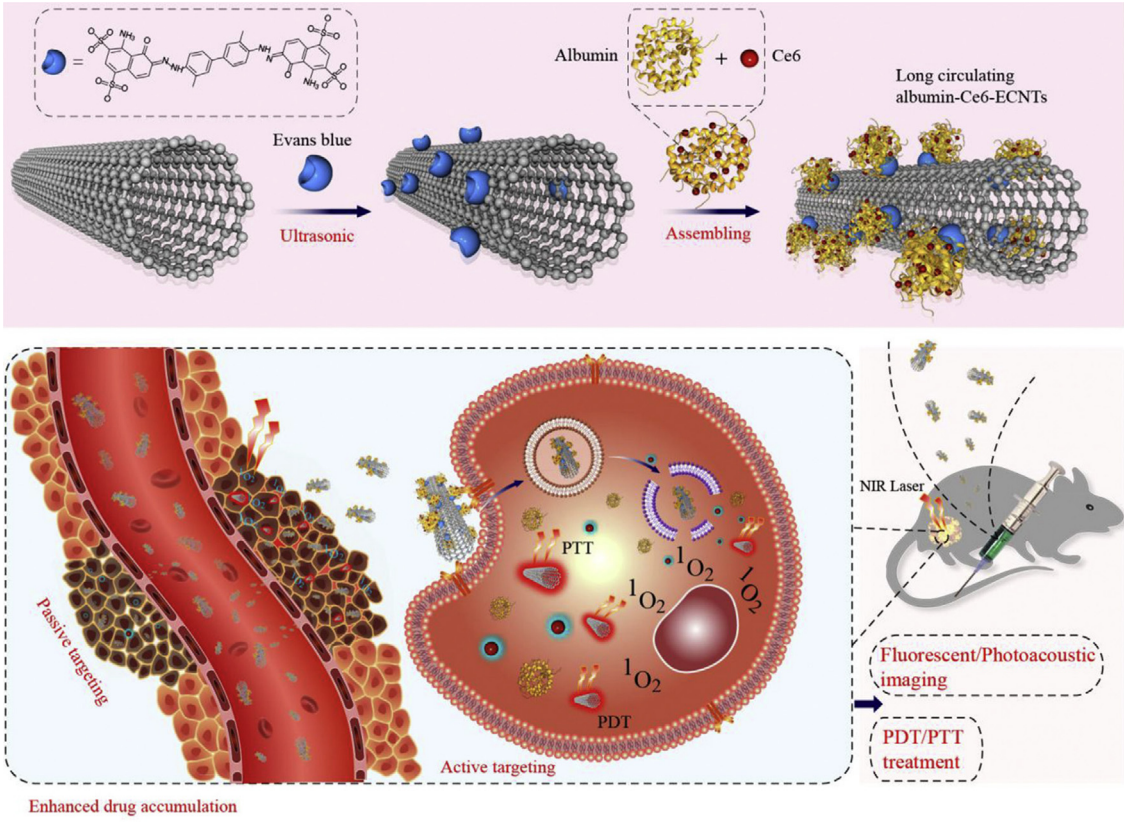

Figure 18 Synthesis of SWCNT-derived NIRF/PAI agent with the combination of PTT and PDT therapies (Adapted from the Ref. 126 with permission. Copyright © 2016 Elsevier Ltd.).

Many of dual-modality OFI/SPECT probes reported were dual labelled antibodies[98–100]. For example, Hekman et al.[101] reported a dual labeled antibody, ^{111}In-DTPA-labetuzumab-IRDye800CW, for detection of pulmonary micro-metastases in a mouse model. Labetuzumab, a humanized monoclonal antibody, was selected as the targeting group for tumor colonies overexpressing carcinoembryonic antigen (CEA). The probe was able to detect tumor metastases at submillimeter sizes not visible to the naked eye in both SPECT and fluorescence imaging (Fig. 16)[101]. Moreover, fluorescence imaging-guided surgery identified more pulmonary nodule lesions than did preoperative SPECT/CT imaging and facilitated a complete removal of tumor lesions. Colocalization of dual-modal images helps to accurately detect small metastatic tumors. The simultaneous consideration of preoperative and intraoperative imaging techniques provides a better localization and assists with complete resection of tumor lesions[101]. Besides antibodies, some small-size biomolecules, such as peptides[102], short RNA sequences[103], and lipopolysaccharides[104], could also be used as targeting groups to construct dual-labelled OFI/SPECT imaging probes.

Notably, lysine-based linker is popular in design of dual-modality OFI/SPECT probes to bring SPECT tracers, NIR fluorophores, and targeting groups together[105–107]. Recently, Dong et al.[108] reported a lysine-centered dual-modality OFI/SPECT probe ^{99m}Tc-HYNIC-lysine(Cy5.5)-PEG$_4$-biotin. A two-step pre-targeting strategy was adopted. Avidin, the pretargeting agent, was injected to the colon tumor grafted mice 4 h before the injection of the dual-modality probe to allow sufficient enrichment of avidin molecules on tumor surface. The probe contains a biotin moiety and the high affinity between avidin and biotin ensured high tumor binding specificity and gave high tumor-to-background contrast[108]. This two-step pre-targeting strategy avoids directly labelling of large biomacromolecules and a potential mismatch between long accumulation time required for enrichment in the target of interest and the short half-lives of PET/SPECT radionuclei; therefore, the probe would provide better image quality with less artifacts, a favorable feature for potential clinical application.

Compared with dual-modality OFI/PET, the fact that more dual-modality OFI/SPECT agents were based on nanoassemblies or nanoparticles such as liposomes[109], polymeric micelles[110], polymeric nanoparticles[111], and cerasomes[112] (Supplementary Information Table S6) was likely because they show better compatibility between *in vivo* pharmakinetic profiles and relatively longer half-lives of many SPECT radioisotopes (Table 1). The larger sizes of nanoparticles also allow for the construction of more complex imaging agents such as trimodality OFI/SPECT/MRI probes[109,111]. Notably, a dual-modality NIRF/SPECT imaging agent, ICG-^{99m}Tc-nanocolloid, has advanced into clinical trials for preoperative mapping of sentinel lymph nodes (SLN) and subsequent surgical removal under guidance of intraoperative NIR fluorescence imaging[113]. The ICG-^{99m}Tc-nanocolloid was prepared from self-assembly of ^{99m}Tc-labelled nanosized human albumin particles (^{99m}Tc-nanocolloid) and FDA approved NIR dye ICG. Compared with the traditional use of ^{99m}Tc-nanocolloid alone,

employment of the dual-labelled nanocolloid reduces false-negative rates of SLN detection, particularly in cases of complex lymphatic drainage when tumors are located in the head and neck region[113].

Certain metal ions utilized for SPECT, PET, and MRI imaging share the same chelators (Table 1), for example, DOTA can form chelates with ^{64}Cu and ^{68}Ga for PET, ^{111}In for SPECT, and Gd (III) for MRI[109]. Therefore, dual-modality OFI/SPECT, OFI/PET, and OFI/MRI probes can be conveniently derived from the same DOTA containing precursor with fluorescence reporting groups. Since SPECT technique is less expensive and more available than PET, SPECT radioisotope could be used initially to evaluate the biodistribution and efficacy of the dual-modality probe, and then substituted by a PET radioisotope to achieve better sensitivity and less radiation exposure in a later translational research.

3.5. *Dual-modality OFI/PAI imaging probes*

Dual-modality OFI/PAI imaging probes, noted for their capability of utilization of multiple endogenous and exogenous PAI contrast agents in a multiplexing manner (MSOT) with fluorescence imaging, offer a robust, noninvasive, and sensitive approach to achieve both anatomical and functional imaging[114]. There are several advantages for a combined use of OFI and PAI. First, poor spatial resolution of OFI in tissue imaging is nicely compensated by the high ultrasonic spatial resolution of PAI. Second, information obtained from 3D volumetric imaging with PAI and superficial images of intraoperical OFI can verify each other for more accurate delineation of disease lesions. Furthermore, endogenous PAI contrast agents (*e.g.*, hemoglobin, melanin, water or lipids) can provide additional anatomical and functional imaging of vascularization, oxygen levels, and morphological details. Generally, there are two major classes of dual-modality OFI/PAI probes depending upon whether both signals are generated from a single fluorophore or different fluorescence and PAI contrast agents.

A dual-modality OFI/PAI probe can be constructed from a single fluorophore[114,115]. Generally, NIR dyes with a high molar extinction coefficient and a moderate fluorescence quantum yield are selected as the fluorophore for better tissue penetration. The moderate quantum yield is required to ensure the generation of modest signals for both modalities, since two signal generation processes of OFI and PAI compete with each other for energy absorption from a NIR laser. For example, ICG, the only FDA-approved NIR fluorescence dye, has been investigated as a dual-functional OFI/PAI probe to image sentinel lymph nodes, lymphatic vessels, and the course and flow of lymphatic vessels in combined NIRF and MSOT imaging studies[116]. However, ICG may be disadvantageous because of its short clearance time, relatively low photostability, and high-binding to plasma proteins. Recently, ICG-loaded nanoprobes were developed to obtain improved stability and longer circulation times during dual modality OFI/PAI imaging of different tumors[46,117,118]. Beziere et al.[118] reported that PEGylated liposome-ICG consisting of entirely clinically-approved material showed great potential as an imaging agent for perfusion investigations of vascular permeability and lymphatic system flow. In a separate study, Ermolayev et al.[46] demonstrated combined use of external liposomal ICG (lipo-ICG) for studies of tumor perfusion dynamics and for tracking endogenous oxygenated (HbO_2) and deoxygenated haemoglobin (Hb) in a breast tumor model using the volumetric MSOT (vMSOT) technique. The major blood vessels identified in 3D vMSOT imaging was then verified by comparison of 2D cross-section images from noninvasive 3D imaging data using haematoxylin-eosin staining (H&E) and planar NIRF imaging of a tumor cryo-section (Fig. 17). The well-matched images from the two different modalities suggest promising potential of the dual-modality NIRF/MSOT probe in noninvasive preoperational diagnosis and NIRF or vMSOT guided surgery[46]. Functionalization of liposome-based ICG nanoprobe with targeted groups (*e.g.*, mAbs) and drugs (*e.g.*, DOX) for tumor chemotherapy was also reported[119]. Aside from ICG, other NIR dyes, such as Cy7 (CDnir7 in Fig. 1)[114], squaraine dye (Usq)[120], croconaine dye (CR780)[121], were also explored as contrasting fluorophores in dual-modality NIR/PAI imaging. Among them, CDnir7 is an NIR dye identified from high-throughput screening specifically for targeting macrophages with potential use in *in vivo* imaging of inflammation[114]. The squaraine dye (Usq) functioned as an activatable probe, which reacts selectively with bioaminothiols inside the body and triggers fluorescence/PA signal changes indicating their levels[120]. PEGlyated CR780 could be self-assembled into nanoparticles with enhanced tumor accumulation, suitable for dual-modality OFI/PAI imaging-guided PTT in cancer theranostic[121].

Though structurally simple, single-fluorophore based OFI/PAI agents have competing signal strength between each imaging modality, which may limit their application. Alternatively, dual-labelling strategy adopting independent fluorescence reporting group and contrasting agent for PAI (*e.g.*, Au nanorods, carbon nanotubes, or an additional NIR dye) can be used for the design of dual-modality OFI/PAI agents. Recently, Guan et al.[122] made core-shell nanoparticles adopting an Au nanorod (AuNR) core and a liposomal ICG shell for PAI and NIRF imaging, respectively[123]. The dual-labelled nanoprobe elicited enhanced PAI signals during preoperative liver cancer diagnosis, which ICG alone was not able to achieve. Moreover, the formation of liposomal ICT also significantly improved stability of ICG for fluorescence imaging. The probe showed promise during both preoperative liver cancer detection and fluorescence-guided resection in a mice xenograft tumor model. In another report, ICG loaded silica-AuNR nanoparticles were used for dual-modality OFI/PAI imaging on both tumor and ischemia mice models[124]. AuNR acted as the core of the nanoparticles. The silica shell functioned as the spacer layer to avoid ICG fluorescence quenching by AuNR. Since AuNR could also be used as CT contrast agent due to its efficient attenuation of X-ray, it is also possible to synthesize a tri-modal OFI/PAI/CT nanoprobe containing AuNR that has multiple therapeutic functions[125]. In addition to AuNR, carbon nanotube could also be integrated into a dual-modality OFI/PAI probe as a PAI contrast agent. Recently, Xie et al.[126] reported a long circulation single wall carbon nanotube (SWCNT) derived NIRF/PAI agent for dual photodynamic therapy (PDT) and photothermal therapy (PTT). To construct the multiple functional probe, SWCNT was first non-covalently attached with Evans blue (EB) molecules on its surface as the sites for further functionalization. The EB-binding sites were then loaded with serum albumin for further attachment of chlorin e6, a widely used photosensitizer for PDT which functions as the fluorescence reporting group (Fig. 18)[126]. The targeting capability was achieved by serum albumin for the albumin receptor gp60 and SPARC on cancer cell surface. This SWCNT-based probe was demonstrated improved efficacy during imaging-guided PDT/PTT tumor ablation therapy[126].

In summary, the combination of OFI and PAI provides convenient, real-time, and compensatory high-resolution of

anatomical structures as well as functional tissue information, suitable for both preoperational lesion mapping and guidance during intra-operational treatment and integration with therapeutic options, particularly photothermal therapy. Dual-modality OFI/PAI imaging is still in a very early stage of development. Current research mainly focuses on probe development and verification of its imaging utility. Much remains to be learned before potential clinical translations can become possible.

4. Conclusions and prospective

Multimodality fluorescence imaging, which combines fluorescence imaging with other imaging modalities, has emerged as a powerful tool for improving sensitivity and accuracy, critical in improved disease diagnosis and treatment (Supplementary Information Tables S2–S7). The improvements in imaging techniques, instrumentation, contrast materials and synthetic methodology will continue to push the boundaries of multimodality imaging methods and probe development. Optical imaging combined with other new imaging modalities is certainly promising, but what ultimately drives the future multimodality probe development is emerging and unmet clinical needs, which include but not limited to imaging-guided surgery, oncology, neurological disease, and personalized medicine. So far, no imaging probe intended for use in dual or multi-modality imaging has been approved by the FDA for clinical use. Most of current probes were developed and investigated for the preclinical biomedical research field, in which information from both deep tissue and superficial biochemical imaging was required or needed to be verified from each other. The question whether one plus one (a single probe with dual-modality) is better than two (a mixture of two probes) has yet to be carefully examined for the purpose of future translation to the clinic.

We have discussed the prospectives for each specific combination of multimodality fluorescence imaging probes. Challenges faced in a multimodality optical fluorescence probe design are tremendous. The challenges are not only dependent on the physical properties of contrast agents and the biocompatibility of the materials, but also associated with the nature of the probe's construction: a small molecule based probe or a nanoprobe. When we consider distinct differences in the sensitivity and the temporal or spatial resolution of any other imaging modality used, an additional layer of complexity is added. More complexity is added when targeting groups, activation or trigger group, and/or therapeutic functions are included. It is not an easy task to select the best combinations of materials and contrast agents, to find the methods to assemble them, and to achieve optimal pharmacokinetics properties (absorption, distribution, metabolism, excretion) and toxicity profiles with also excellent target accumulation. The process will require systems engineering and multiple rounds of meticulous optimization. All these efforts would potentially lead to the discovery of novel theranostic agents for earlier and more accurate diagnoses and cost-efficient intervention to give patients longer and higher quality lives.

Acknowledgments

The work was supported by the National Science Foundation of China (No. 21577037 to Kaiyan Lou), and East China University of Science and Technology (Grant No. YC0140101, start-up funds to Wei Wang).

Appendix A. Supporting information

Supplementary data associated with this article can be found in the online version at https://doi.org/10.1016/j.apsb.2018.03.010.

References

1. Alberti C. From molecular imaging in preclinical/clinical oncology to theranostic applications in targeted tumor therapy. *Eur Rev Med Pharmacol Sci* 2012;**16**:1925–33.
2. Bu L, Shen B, Cheng Z. Fluorescent imaging of cancerous tissues for targeted surgery. *Adv Drug Deliv Rev* 2014;**76**:21–38.
3. Louie A. Multimodality imaging probes: design and challenges. *Chem Rev* 2010;**110**:3146–95.
4. James ML, Gambhir SS. A molecular imaging primer: modalities, imaging agents, and applications. *Physiol Rev* 2012;**92**:897–965.
5. Gao H. Progress and perspectives on targeting nanoparticles for brain drug delivery. *Acta Pharm Sin B* 2016;**6**:268–86.
6. Lee SY, Jeon SI, Jung S, Chung IJ, Ahn CH. Targeted multimodal imaging modalities. *Adv Drug Deliv Rev* 2014;**76**:60–78.
7. Gioux S, Choi HS, Frangioni JV. Image-guided surgery using invisible near-infrared light: fundamentals of clinical translation. *Mol Imaging* 2010;**9**(5)237–55.
8. Xu G, Zeng S, Zhang B, Swihart MT, Yong KT, Prasad PN. New generation cadmium-free quantum dots for biophotonics and nanomedicine. *Chem Rev* 2016;**116**:12234–327.
9. Michalet X, Pinaud FF, Bentolila LA, Tsay JM, Doose S, Li JJ, et al. Quantum dots for live cells, *in vivo* imaging, and diagnostics. *Science* 2005;**307**:538–44.
10. Park YI, Lee KT, Suh YD, Hyeon T. Upconverting nanoparticles: a versatile platform for wide-field two-photon microscopy and multimodal *in vivo* imaging. *Chem Soc Rev* 2015;**44**:1302–17.
11. Liu J, Liu C, He W. Fluorophores and their applications as molecular probes in living cells. *Curr Org Chem* 2013;**17**:564–79.
12. Rodriguez EA, Campbell RE, Lin JY, Lin MZ, Miyawaki A, Palmer AE, et al. The growing and glowing toolbox of fluorescent and photoactive proteins. *Trends Biochem Sci* 2017;**42**:111–29.
13. Kwok RT, Leung CW, Lam JW, Tang BZ. Biosensing by luminogens with aggregation-induced emission characteristics. *Chem Soc Rev* 2015;**44**:4228–38.
14. Mei J, Leung NL, Kwok RT, Lam JW, Tang BZ. Aggregation-induced emission: together we shine, united we soar!. *Chem Rev* 2015;**115**:11718–940.
15. Ntziachristos V, Bremer C, Weissleder R. Fluorescence imaging with near-infrared light: new technological advances that enable *in vivo* molecular imaging. *Eur Radiol* 2003;**13**:195–208.
16. Koo V, Hamilton PW, Williamson K. Non-invasive *in vivo* imaging in small animal research. *Cell Oncol* 2006;**28**:127–39.
17. Fayed TA. Extension of fluorescence response to the near-IR region. In: Geddes CD, editor. *Reviews in fluorescence 2009*. New York: Springer; 2011. p. 75–111.
18. Tong H, Lou K, Wang W. Near-infrared fluorescent probes for imaging of amyloid plaques in Alzheimer's disease. *Acta Pharm Sin B* 2015;**5**:25–33.
19. Schaafsma BE, Mieog JS, Hutteman M, van der Vorst JR, Kuppen PJ, Löwik CW, et al. The clinical use of indocyanine green as a near-infrared fluorescent contrast agent for image-guided oncologic surgery. *J Surg Oncol* 2011;**104**:323–32.
20. Namikawa T, Sato T, Hanazaki K. Recent advances in near-infrared fluorescence-guided imaging surgery using indocyanine green. *Surg Today* 2015;**45**:1467–74.
21. Adams A, Mourik JE, van der Voort M, Pearlman PC, Nielsen T, Mali WP, et al. Estimation of detection limits of a clinical fluorescence optical mammography system for the near-infrared fluorophore IRDye800CW: phantom experiments. *J Biomed Opt* 2012;**17**:076022.

22. Hemmer E, Benayas A, Légaré F, Vetrone F. Exploiting the biological windows: current perspectives on fluorescent bioprobes emitting above 1000 nm. *Nanoscale Horiz* 2016;**1**:168–84.
23. Qin MY, Yang XQ, Wang K, Zhang XS, Song JT, Yao MH, et al. *In vivo* cancer targeting and fluorescence-CT dual-mode imaging with nanoprobes based on silver sulfide quantum dots and iodinated oil. *Nanoscale* 2015;**7**:19484–92.
24. Kamimura M, Saito R, Hyodo H, Tsuji K, Umeda IO, Fujii H, et al. Over-1000 nm near-infrared fluorescence and SPECT/CT dual-modal *in vivo* imaging based on rare-earth doped ceramic nanophosphors. *J Photopolym Sci Tec* 2016;**29**:525–32.
25. Pan Q, Ye S, Yang D, Qiu J, Dong G. Multifunctional magnetic-fluorescent Ni-doped $ZnAl_2O_4$ nanoparticles with second biological NIR window fluorescence. *Mater Res Bull* 2017;**93**:310–7.
26. Li C, Shi G. Carbon nanotube-based fluorescence sensors. *J Photochem Photobiol C* 2014;**19**:20–34.
27. Liu Y, Ai K, Lu L. Nanoparticulate X-ray computed tomography contrast agents: from design validation to *in vivo* applications. *Acc Chem Res* 2012;**45**:1817–27.
28. Hyafil F, Cornily JC, Feig JE, Gordon R, Vucic E, Amirbekian V, et al. Noninvasive detection of macrophages using a nanoparticulate contrast agent for computed tomography. *Nat Med* 2007;**13**:636–41.
29. Popovtzer R, Agrawal A, Kotov NA, Popovtzer A, Balter J, Carey TE, et al. Targeted gold nanoparticles enable molecular CT imaging of cancer. *Nano Lett* 2008;**8**:4593–6.
30. Li J, Chaudhary A, Chmura SJ, Pelizzari C, Rajh T, Wietholt C, et al. A novel functional CT contrast agent for molecular imaging of cancer. *Phys Med Biol* 2010;**55**:4389–97.
31. Kim D, Jeong YY, Jon S. A drug-loaded aptamer-gold nanoparticle bioconjugate for combined CT imaging and therapy of prostate cancer. *ACS Nano* 2010;**4**:3689–96.
32. Lu YC, Yang CX, Yan XP. Radiopaque tantalum oxide coated persistent luminescent nanoparticles as multimodal probes for *in vivo* near-infrared luminescence and computed tomography bioimaging. *Nanoscale* 2015;**7**:17929–37.
33. Prasad PV. *Magnetic resonance imaging: methods and biologic applications*. Totowa: Humana Press Inc; 447.
34. Takaoka Y, Sakamoto T, Tsukiji S, Narazaki M, Matsuda T, Tochio H, et al. Self-assembling nanoprobes that display off/on ^{19}F nuclear magnetic resonance signals for protein detection and imaging. *Nat Chem* 2009;**1**:557–61.
35. Tirotta I, Dichiarante V, Pigliacelli C, Cavallo G, Terraneo G, Bombelli FB, et al. ^{19}F magnetic resonance imaging (MRI): from design of materials to clinical applications. *Chem Rev* 2015;**115**:1106–29.
36. Yuan Y, Sun H, Ge S, Wang M, Zhao H, Wang L, et al. Controlled intracellular self-assembly and disassembly of ^{19}F nanoparticles for MR imaging of caspase 3/7 in zebrafish. *ACS Nano* 2015;**9**:761–8.
37. Ametamey SM, Honer M, Schubiger PA. Molecular imaging with PET. *Chem Rev* 2008;**108**:1501–16.
38. Kelloff GJ, Hoffman JM, Johnson B, Scher HI, Siegel BA, Cheng EY, et al. Progress and promise of FDG-PET imaging for cancer patient management and oncologic drug development. *Clin Cancer Res* 2005;**11**:2785–808.
39. Chiaravalloti A, Danieli R, Lacanfora A, Palumbo B, Caltagirone C, Schillaci O. Usefulness of 18F florbetaben in diagnosis of Alzheimer's disease and other types of dementia. *Curr Alzheimer Res* 2017;**14**:154–60.
40. Pimlott SL, Sutherland A. Molecular tracers for the PET and SPECT imaging of disease. *Chem Soc Rev* 2011;**40**:149–62.
41. Wadas TJ, Wong EH, Weisman GR, Anderson CJ. Coordinating radiometals of copper, gallium, indium, yttrium, and zirconium for PET and SPECT imaging of disease. *Chem Rev* 2010;**110**:2858–902.
42. Yao J, Wang LV. Photoacoustic tomography: fundamentals, advances and prospects. *Contrast Media Mol Imaging* 2011;**6**:332–45.
43. Wang LV, Hu S. Photoacoustic tomography: *in vivo* imaging from organelles to organs. *Science* 2012;**335**:1458–62.
44. Gujrati V, Mishra A, Ntziachristos V. Molecular imaging probes for multi-spectral optoacoustic tomography. *Chem Commun* 2017;**53**:4653–72.
45. Ntziachristos V, Razansky D. Molecular imaging by means of multispectral optoacoustic tomography (MSOT). *Chem Rev* 2010;**110**:2783–94.
46. Ermolayev V, Dean-Ben XL, Mandal S, Ntziachristos V, Razansky D. Simultaneous visualization of tumour oxygenation, neovascularization and contrast agent perfusion by real-time three-dimensional optoacoustic tomography. *Eur Radiol* 2016;**26**:1843–51.
47. Miao Q, Pu K. Emerging designs of activatable photoacoustic probes for molecular imaging. *Bioconjugate Chem* 2016;**27**:2808–23.
48. Lutzweiler C, Razansky D. Optoacoustic imaging and tomography: reconstruction approaches and outstanding challenges in image performance and quantification. *Sensors* 2013;**13**:7345–84.
49. Huang H, Dunne M, Lo J, Jaffray DA, Allen C. Comparison of computed tomography- and optical image-based assessment of liposome distribution. *Mol Imaging* 2013;**12**:148–60.
50. Liu Y, Tian GF, He XW, Li WY, Zhang YK. Microwave-assisted one-step rapid synthesis of near-infrared gold nanoclusters for NIRF/CT dual-modal bioimaging. *J Mater Chem B* 2016;**4**:1276–83.
51. Chen J, Yang XQ, Meng YZ, Qin MY, Yan DM, Qian Y, et al. Reverse microemulsion-mediated synthesis of Bi_2S_3-QD@SiO_2-PEG for dual modal CT-fluorescence imaging *in vitro* and *in vivo*. *Chem Commun* 2013;**49**:11800–2.
52. Zhang J, Li C, Zhang X, Huo SD, Jin SB, An FF, et al. *In vivo* tumor-targeted dual-modal fluorescence/CT imaging using a nanoprobe co-loaded with an aggregation-induced emission dye and gold nanoparticles. *Biomaterials* 2015;**42**:103–11.
53. Zeng S, Zhou R, Zheng X, Wu L, Hou X. Mono-dispersed Ba^{2+}-doped nano-hydroxyapatite conjugated with near-infrared Cu-doped CdS quantum dots for CT/fluorescence bimodal targeting cell imaging. *Microchem J* 2017;**134**:41–8.
54. Caravan P, Ellison JJ, McMurry TJ, Lauffer RB. Gadolinium(III) chelates as MRI contrast agents: structure, dynamics, and applications. *Chem Rev* 1999;**99**:2293–352.
55. Guo K, Berezin MY, Zheng J, Akers W, Lin F, Teng B, et al. Near infrared-fluorescent and magnetic resonance imaging molecular probe with high T_1 relaxivity for *in vivo* multimodal imaging. *Chem Commun* 2010;**46**:3705–7.
56. Yamane T, Hanaoka K, Muramatsu Y, Tamura K, Adachi Y, Miyashita Y, et al. Method for enhancing cell penetration of Gd^{3+}-based MRI contrast agents by conjugation with hydrophobic fluorescent dyes. *Bioconjugate Chem* 2011 2227–36.
57. Harrison VS, Carney CE, MacRenaris KW, Waters EA, Meade TJ. Multimeric near IR-MR contrast agent for multimodal *in vivo* imaging. *J Am Chem Soc* 2015;**137**:9108–16.
58. Dong D, Jing X, Zhang X, Hu X, Wu Y, Duan C. Gadolinium(III)-fluorescein complex as a dual modal probe for MRI and fluorescence zinc sensing. *Tetrahedron* 2012;**68**:306–10.
59. Wang Y, Song R, Feng H, Guo K, Meng Q, Chi H, et al. Visualization of fluoride ions *in vivo* using a gadolinium(III)-coumarin complex-based fluorescence/MRI dual-modal probe. *Sensors* 2016;**16**:2165.
60. Wang Y, Song R, Guo K, Meng Q, Zhang R, Kong X, et al. A Gadolinium(III) complex based dual-modal probe for MRI and fluorescence sensing of fluoride ions in aqueous medium and *in vivo*. *Dalton Trans* 2016;**45**:17616–23.
61. Hu H, Sheng Y, Ye M, Qian Y, Tang J, Shen Y. A porphyrin-based magnetic and fluorescent dual-modal nanoprobe for tumor imaging. *Polymer* 2016;**88**:94–101.
62. Zhu FP, Chen GT, Wang SJ, Liu Y, Tang YX, Tian Y, et al. Dual-modality imaging probes with high magnetic relaxivity and near-infrared fluorescence based highly aminated mesoporous silica nanoparticles. *J Nanomater* 2016;**2016**:6502127.

63. Lee N, Hyeon T. Designed synthesis of uniformly sized iron oxide nanoparticles for efficient magnetic resonance imaging contrast agents. *Chem Soc Rev* 2012;**41**:2575–89.
64. Yan X, Song X, Wang Z. Construction of specific magnetic resonance imaging/optical dual-modality molecular probe used for imaging angiogenesis of gastric cancer. *Artif Cells Nanomed Biotechnol* 2017;**45**:399–403.
65. Qiao H, Wang Y, Zhang R, Gao Q, Liang X, Gao L, et al. MRI/optical dual-modality imaging of vulnerable atherosclerotic plaque with an osteopontin-targeted probe based on Fe_3O_4 nanoparticles. *Biomaterials* 2017;**112**:336–45.
66. Chen Q, Shang W, Zeng C, Wang K, Liang X, Chi C, et al. Theranostic imaging of liver cancer using targeted optical/MRI dual-modal probes. *Oncotarget* 2017;**8**:32741–51.
67. Nakamura T, Sugihara F, Matsushita H, Yoshioka Y, Mizukami S, Kikuchi K. Mesoporous silica nanoparticles for ^{19}F magnetic resonance imaging, fluorescence imaging, and drug delivery. *Chem Sci* 2015;**6**:1986–90.
68. Guo C, Xu M, Xu S, Wang L. Multifunctional nanoprobes for both fluorescence and ^{19}F magnetic resonance imaging. *Nanoscale* 2017;**9**:7163–8.
69. Goswami LN, Khan AA, Jalisatgi SS, Hawthorne MF. Synthesis and *in vitro* assessment of a bifunctional closomer probe for fluorine (^{19}F) magnetic resonance and optical bimodal cellular imaging. *Chem Commun* 2014;**50**:5793–5.
70. Liu X, Jiang H, Ye J, Zhao C, Gao S, Wu C, et al. Nitrogen-doped carbon quantum dot stabilized magnetic iron oxide nanoprobe for fluorescence, magnetic resonance, and computed tomography triple-modal *in vivo* bioimaging. *Adv Funct Mater* 2016;**26**:8694–706.
71. Dong W, Li Y, Niu D, Ma Z, Liu X, Gu J, et al. A simple route to prepare monodisperse Au NP-decorated, dye-doped, superparamagnetic nanocomposites for optical, MR, and CT trimodal imaging. *Small* 2013;**9**:2500–8.
72. Xue S, Wang Y, Wang M, Zhang L, Du X, Gu H, et al. Iodinated oil-loaded, fluorescent mesoporous silica-coated iron oxide nanoparticles for magnetic resonance imaging/computed tomography/fluorescence trimodal imaging. *Int J Nanomedicine* 2014;**9**:2527–38.
73. Yang G, Gong H, Liu T, Sun X, Cheng L, Liu Z. Two-dimensional magnetic WS_2@Fe_3O_4 nanocomposite with mesoporous silica coating for drug delivery and imaging-guided therapy of cancer. *Biomaterials* 2015;**60**:62–71.
74. Wu B, Wan B, Lu ST, Deng K, Li XQ, Wu BL, et al. Near-infrared light-triggered theranostics for tumor-specific enhanced multimodal imaging and photothermal therapy. *Int J Nanomed* 2017 4467–78.
75. Han L, Xia JM, Hai X, Shu Y, Chen XW, Wang JH. Protein-stabilized gadolinium oxide-gold nanoclusters hybrid for multimodal imaging and drug delivery. *ACS Appl Mater Interfaces* 2017;**9**:6941–9.
76. Deng X, Dai Y, Liu J, Zhou Y, Ma P, Cheng Z, et al. Multifunctional hollow CaF_2:yb^{3+}/Er^{3+}/Mn^{2+}-poly(2-aminoethyl methacrylate) microspheres for Pt(IV) pro-drug delivery and tri-modal imaging. *Biomaterials* 2015;**50**:154–63.
77. An FF, Chan M, Kommidi H, Ting R. Dual PET and near-infrared fluorescence imaging probes as tools for imaging in oncology. *AJR Am J Roentgenol* 2016;**207**:266–73.
78. Seibold U, Wängler B, Schirrmacher R, Wängler C. Bimodal imaging probes for combined PET and OI: recent developments and future directions for hybrid agent development. *Biomed Res Int* 2014;**2014**:153741.
79. Ghosh SC, Azhdarinia A. Advances in the development of multimodal imaging agents for nuclear/near-infrared fluorescence imaging. *Curr Med Chem* 2015;**22**:3390–404.
80. Preshlock S, Tredwell M, Gouverneur V. ^{18}F-Labeling of arenes and heteroarenes for applications in positron emission tomography. *Chem Rev* 2016;**116**:719–66.
81. Summer D, Grossrubatscher L, Petrik M, Michalcikova T, Novy Z, Rangger C, et al. Developing targeted hybrid imaging probes by chelator scaffolding. *Bioconjugate Chem* 2017;**28**:1722–33.
82. Boswell CA, Sun XK, Niu WJ, Weisman GR, Wong EH, Rheingold AL, et al. Comparative *in vivo* stability of copper-64-labeled cross-bridged and conventional tetraazamacrocyclic complexes. *J Med Chem* 2004;**47**:1465–74.
83. Gaedicke S, Braun F, Prasad S, Machein M, Firat E, Hettich M, et al. Noninvasive positron emission tomography and fluorescence imaging of $CD133^+$ tumor stem cells. *Proc Natl Acad Sci U S A* 2014;**111**:E692–701.
84. Ghosh SC, Ghosh P, Wilganowski N, Robinson H, Hall MA, Dickinson G, et al. Multimodal chelation platform for near-infrared fluorescence/nuclear imaging. *J Med Chem* 2013;**56**:406–16.
85. Hendricks JA, Keliher EJ, Wan D, Hilderbrand SA, Weissleder R, Mazitschek R. Synthesis of [^{18}F] BODIPY: bifunctional reporter for hybrid optical/positron emission tomography imaging. *Angew Chem Int Ed Engl* 2012;**51**:4603–6.
86. Rodriguez EA, Wang Y, Crisp JL, Vera DR, Tsien RY, Ting R. New dioxaborolane chemistry enables [^{18}F]-positron-emitting, fluorescent [^{18}F]-multimodality biomolecule generation from the solid phase. *Bioconjugate Chem* 2016;**27**:1390–9.
87. Steiner M, Neri D. Antibody-radionuclide conjugates for cancer therapy: historical considerations and new trends. *Clin Cancer Res* 2011;**17**:6406–16.
88. Zhang H, Desai P, Koike Y, Houghton J, Carlin S, Tandon N, et al. Dual-modality imaging of prostate cancer with a fluorescent and radiogallium-labeled gastrin-releasing peptide receptor antagonist. *J Nucl Med* 2017;**58**:29–35.
89. Sun Y, Ma X, Cheng K, Wu B, Duan J, Chen H, et al. Strained cyclooctyne as a molecular platform for construction of multimodal imaging probes. *Angew Chem Int Ed Engl* 2015;**54**:5981–4.
90. Sun L, Ding J, Xing W, Gai Y, Sheng J, Zeng D. Novel strategy for preparing dual-modality optical/PET imaging probes *via* photo-click chemistry. *Bioconjugate Chem* 2016;**27**:1200–4.
91. Paulus A, Maenen M, Drude N, Nascimento EB, van Marken Lichtenbelt WD, Mottaghy FM, et al. Synthesis, radiosynthesis and *in vitro* evaluation of ^{18}F-Bodipy-C_{16}/triglyceride as a dual modal imaging agent for brown adipose tissue. *PLoS One* 2017;**12**: e0182297.
92. An FF, Kommidi H, Chen N, Ting R. A conjugate of pentamethine cyanine and ^{18}F as a positron emission tomography/near-infrared fluorescence probe for multimodality tumor imaging. *Int J Mol Sci* 2017;**18**:1214.
93. Wang Y, An FF, Chan M, Friedman B, Rodriguez EA, Tsien RY, et al. ^{18}F-positron-emitting/fluorescent labeled erythrocytes allow imaging of internal hemorrhage in a murine intracranial hemorrhage model. *J Cereb Blood Flow Metab* 2017;**37**:776–86.
94. Kommidi H, Guo H, Chen N, Kim D, He B, Wu AP, et al. An [^{18}F]-positron-emitting, fluorescent, cerebrospinal fluid probe for imaging damage to the brain and spine. *Theranostics* 2017;**7**:2377–91.
95. Chansaenpak K, Wang H, Wang M, Giglio B, Ma X, Yuan H, et al. Synthesis and evaluation of [^{18}F]-ammonium BODIPY dyes as potential positron emission tomography agents for myocardial perfusion imaging. *Chemistry* 2016;**22**:12122–9.
96. Liu S, Li D, Shan H, Gabbaï FP, Li Z, Conti PS. Evaluation of ^{18}F-labeled BODIPY dye as potential PET agents for myocardial perfusion imaging. *Nucl Med Biol* 2014;**41**:120–6.
97. Shimojo M, Higuchi M, Suhara T, Sahara N. Imaging multimodalities for dissecting Alzheimer's disease: advanced technologies of positron emission tomography and fluorescence imaging. *Front Neurosci* 2015;**9**:482.
98. Boonstra MC, van Driel PB, van Willigen DM, Stammes MA, Prevoo HA, Tummers QR, et al. uPAR-targeted multimodal tracer for pre- and intraoperative imaging in cancer surgery. *Oncotarget* 2015;**6**:14260–73.

99. Lüutje S, Rijpkema M, Franssen GM, et al. Dual-modality image-guided surgery of prostate cancer with a radiolabeled fluorescent anti-PSMA monoclonal antibody. *J Nucl Med* 2014;**55**:995–1001.
100. Rijpkema M, Oyen WJ, Bos D, Franssen GM, Goldenberg DM, Boerman OC. SPECT- and fluorescence image-guided surgery using a dual-labeled carcinoembryonic antigen-targeting antibody. *J Nucl Med* 2014;**55**:1519–24.
101. Hekman MC, Rijpkema M, Bos DL, Oosterwijk E, Goldenberg DM, Mulders PF, et al. Detection of micrometastases using SPECT/fluorescence dual-modality imaging in a CEA-expressing tumor model. *J Nucl Med* 2017;**58**:706–10.
102. Li Z, Zhang G, Shen H, Zhang L, Wang Y. Synthesis and cell uptake of a novel dualmodality ^{188}Re-HGRGD (D) F-CdTe QDs probe. *Talanta* 2011;**85**:936–42.
103. Wang Y, Chen L, Liu X, Cheng D, Liu G, Liu Y, et al. Detection of Aspergillus fumigatus pulmonary fungal infections in mice with ^{99m}Tc-labeled MORF oligomers targeting ribosomal RNA. *Nucl Med Biol* 2013;**40**:89–96.
104. Duheron V, Moreau M, Collin B, Sali W, Bernhard C, Goze C, et al. Dual labeling of lipopolysaccharides for SPECT-CT imaging and fluorescence microscopy. *ACS Chem Biol* 2014;**9**:656–62.
105. Bhushan KR, Misra P, Liu F, Mathur S, Lenkinski RE, Frangioni JV. Detection of breast cancer microcalcifications using a dual-modality SPECT/NIR fluorescent probe. *J Am Chem Soc* 2008;**130**:17648–9.
106. Bunschoten A, Buckle T, Visser NL, Kuil J, Yuan H, Josephson L, et al. Multimodal interventional molecular imaging of tumor margins and distant metastases by targeting $\alpha v\beta 3$ Integrin. *ChemBioChem* 2012;**13**:1039–45.
107. Guo Y, Yuan H, Cho H, Kuruppu D, Jokivarsi K, Agarwal A, et al. High efficiency diffusion molecular retention tumor targeting. *PLoS One* 2013;**8**:e58290.
108. Dong C, Yang S, Shi J, Zhao H, Zhong L, Liu Z, et al. SPECT/NIRF dual modality imaging for detection of intraperitoneal colon tumor with an avidin/biotin pretargeting system. *Sci Rep* 2016;**6**:18905.
109. Mitchell N, Kalber TL, Cooper MS, Sunassee K, Chalker SL, Shaw KP, et al. Incorporation of paramagnetic, fluorescent and PET/SPECT contrast agents into liposomes for multimodal imaging. *Biomaterials* 2013;**34**:1179–92.
110. Zhang R, Huang M, Zhou M, Wen X, Huang Q, Li C, et al. Annexin A5-functionalized nanoparticle for multimodal imaging of cell death. *Mol Imaging* 2013;**12**:183–90.
111. Saatchi K, Soema P, Gelder N, Misri R, McPhee K, Baker JH, et al. Hyperbranched polyglycerols as trimodal imaging agents: design, biocompatibility, and tumor uptake. *Bioconjugate Chem* 2012;**23**:372–81.
112. Jing L, Shi J, Fan D, Li Y, Liu R, Dai Z, et al. ^{177}Lu-labeled cerasomes encapsulating indocyanine green for cancer theranostics. *ACS Appl Mater Interfaces* 2015;**7**:22095–105.
113. KleinJan GH, Bunschoten A, van den Berg NS, Olmos RA, Klop WM, Horenblas S, et al. Fluorescence guided surgery and tracer-dose, fact or fiction?. *Eur J Nucl Med Mol Imaging* 2016;**43**:1857–67.
114. Kang NY, Park SJ, Ang XW, Samanta A, Driessen WH, Ntziachristos V, et al. A macrophage uptaking near-infrared chemical probe CDnir7 for *in vivo* imaging of inflammation. *Chem Commun* 2014;**50**:6589–91.
115. Sim N, Gottschalk S, Pal R, Delbianco M, Degtyaruk O, Razansky D, et al. Wavelength-dependent optoacoustic imaging probes for NMDA receptor visualisation. *Chem Commun* 2015;**51**:15149–52.
116. Kim C, Song KH, Gao F, Gao F, Wang LV. Sentinel lymph nodes and lymphatic vessels: noninvasive dual-modality i*n vivo* mapping by using indocyanine green in rats-volumetric spectroscopic photoacoustic imaging and planar fluorescence imaging. *Radiology* 2010;**255**:442–50.
117. Chen J, Liu C, Zeng G, You Y, Wang H, Gong X, et al. Indocyanine green loaded reduced graphene oxide for *in vivo* photoacoustic/fluorescence dual-modality tumor imaging. *Nanoscale Res Lett* 2016;**11**:85.
118. Beziere N, Lozano N, Nunes A, Salichs J, Queiros D, Kostarelos K, et al. Dynamic imaging of PEGylated indocyanine green (ICG) liposomes within the tumor microenvironment using multi-spectral optoacoustic tomography (MSOT). *Biomaterials* 2015;**37**:415–24.
119. Lozano N, Al-Ahmady ZS, Beziere NS, Ntziachristos V, Kostarelos K. Monoclonal antibody-targeted PEGylated liposome-ICG encapsulating doxorubicin as a potential theranostic agent. *Int J Pharm* 2015;**482**:2–10.
120. Anees P, Joseph J, Sreejith S, Menon NV, Kang Y. Wing-Kwong Yu S, et al. Real time monitoring of aminothiol level in blood using a near-infrared dye assisted deep tissue fluorescence and photoacoustic bimodal imaging. *Chem Sci* 2016;**7**:4110–6.
121. Tang L, Zhang F, Yu F, Sun W, Song M, Chen X, et al. Croconaine nanoparticles with enhanced tumor accumulation for multimodality cancer theranostics. *Biomaterials* 2017;**129**:28–36.
122. Miyata A, Ishizawa T, Kamiya M, Shimizu A, Kaneko J, Ijichi H, et al. Photoacoustic tomography of human hepatic malignancies using intraoperative indocyanine green fluorescence imaging. *PLoS One* 2014;**9**:e112667.
123. Guan T, Shang W, Li H, Yang X, Fang C, Tian J, et al. From detection to resection: photoacoustic tomography and surgery guidance with Indocyanine Green loaded gold nanorod@liposome core-shell nanoparticles in liver cancer. *Bioconjugate Chem* 2017;**28**:1221–8.
124. Peng D, Du Y, Shi Y, Mao D, Jia X, Li H, et al. Precise diagnosis in different scenarios using photoacoustic and fluorescence imaging with dual-modality nanoparticles. *Nanoscale* 2016;**8**:14480–8.
125. Duan S, Yang Y, Zhang C, Zhao N, Xu FJ. NIR-responsive polycationic gatekeeper-cloaked hetero-nanoparticles for multimodal imaging-guided triple-combination therapy of cancer. *Small* 2017;**13**:1603133.
126. Xie L, Wang G, Zhou H, Zhang F, Guo Z, Liu C, et al. Functional long circulating single walled carbon nanotubes for fluorescent/photoacoustic imaging-guided enhanced phototherapy. *Biomaterials* 2016;**103**:219–28.